

Co-regulation of water use and canopy temperature in desert trees

Bryn E. Morgan ^{a,b}, Anna T. Trugman ^{a,b}, Kelly K. Caylor ^{a,b,c}

^a Department of Geography, University of California, Santa Barbara, Santa Barbara, CA, USA

^b Earth Research Institute, University of California, Santa Barbara, Santa Barbara, CA, USA

^c Bren School of Environmental Science and Management, University of California, Santa Barbara, Santa Barbara, CA, USA

ARTICLE INFO

Dataset link: <https://doi.org/10.5281/zenodo.17563443>

Keywords:

Ecohydrology
Stomatal regulation
Canopy temperature
Transpiration
Plant physiology
Water stress

ABSTRACT

Plants employ a range of water-use strategies to withstand limitations in water supply and increases in atmospheric demand. At the same time, water-use strategies alter canopy energy balance, leading to changes in canopy temperature that can impact photosynthesis, creating distinct tradeoffs between water and temperature regulation. However, the extent of these tradeoffs is a key uncertainty in understanding plant responses to hydroclimatic stress. Here, we use a unique dataset of near-surface remotely sensed retrievals of canopy conductance, transpiration, and temperature to assess how desert trees co-regulate their water status and temperature. We leverage a moisture gradient and seasonality in temperature to evaluate species-specific plant responses to both isolated (cool, dry and hot, wet) and combined (hot, dry) water and temperature stress and compare them to reference (cool, wet) conditions. We find that species exhibit different water-use strategies in response to supply- and demand-driven water stress, but exhibit similar responses to thermal stress. Under most conditions, plants face tradeoffs between hydraulic function and avoiding thermal stress. However, when both supply and demand are high, water and canopy temperature regulation can become decoupled. Altogether, our findings reveal two unexpected plant behaviors that may be particularly vulnerable to climate change.

1. Introduction

Plants play a critical role in Earth system functioning by regulating water, carbon, and energy fluxes between the atmosphere and the land surface (Bonan, 2008; Anderegg and Venturas, 2020). Ecosystem function is mediated by the supply of water in the plant root zone and demand for water in the atmosphere (Mencuccini et al., 2019), so how ecosystems respond to climate change will depend on how individual plants regulate their water, carbon, and energy fluxes and how plant interactions scale to ecosystem responses as water supply and demand change (Liu et al., 2020b; Anderegg, 2015; Roman et al., 2015; Sulman et al., 2016; Mrad et al., 2019). As climate change leads to increasing variability in plant-available moisture (Peng et al., 2023; Field et al., 2012), rising temperatures (IPCC, 2023), and increasing atmospheric moisture deficit (Dai, 2006; Douville et al., 2022; Simpson et al., 2024), understanding how plants respond to changes in the supply of and demand for water is critical for predicting ecosystem water use (Jung et al., 2010), carbon uptake (Trugman et al., 2018), and mortality (Anderegg et al., 2013, 2016).

Plants use a variety of strategies to regulate their water use and carbon uptake when water is limited, ranging from more profligate to more conservative responses to dryness (Jones, 1980; Ludlow, 1989). Water status is regulated via stomatal conductance, g_s [$\text{mol m}^{-2} \text{s}^{-1}$],

which is proportional to transpiration. Species that employ more conservative water-use strategies tightly regulate stomatal conductance as available moisture declines to preserve leaf and xylem water potential (Tardieu and Simonneau, 1998). In contrast, more profligate species maintain g_s despite low water availability by investing in drought-tolerant structural strategies (Sperry et al., 2002; Meinzer et al., 2016; Hacke et al., 2001; Jacobsen et al., 2007) that allow them to sustain photosynthesis under drier conditions. At the same time, atmospheric vapor pressure deficit (VPD_a , [kPa]), and, more specifically, the leaf-to-air vapor pressure deficit (VPD_l , [kPa]), which is calculated from leaf temperature, can induce stomatal closure to minimize water loss and avoid loss of xylem tension (Running, 1976; Grossiord et al., 2020; McDowell et al., 2008; Schönbeck et al., 2022). Stomatal conductance—or, at the plant scale, canopy conductance, g_c [$\text{mol m}^{-2} \text{s}^{-1}$]—typically declines as a logarithmic function of increasing VPD_l (Oren et al., 1999; Fig. 1a). Both the degree of this decline – i.e., the sensitivity of g_c to VPD_l (m , [-]) – and the reference conductance when VPD_l is low ($g_{c,\text{ref}}$, [$\text{mol m}^{-2} \text{s}^{-1}$]; Eq. (2)) depend on numerous factors, including water availability (Novick et al., 2016) and species-specific hydraulic strategies (Grossiord et al., 2017). In general, water limitation leads to an increase in hydraulic regulation in response to elevated VPD_l .

* Correspondence to: Department of Civil and Environmental Engineering, Massachusetts Institute of Technology, Cambridge, MA, USA.
E-mail address: brynmorgan@ucsb.edu (B.E. Morgan).

(i.e., m) and a decrease in $g_{c,\text{ref}}$ (Novick et al., 2016), all else being equal. However, higher sensitivity to VPD_l is typically associated with higher $g_{c,\text{ref}}$ (Cunningham, 2004; Berger-Landefeldt, 1936), so a stronger response to VPD_l does not necessarily indicate lower g_c at a given VPD_l, particularly when both supply and demand are either low or high. Moreover, sensitivity to both moisture availability and VPD_l can vary widely, even within the same species, plant functional type, or ecosystem (Feng et al., 2019; Anderegg et al., 2018; Anderegg, 2015; Choat et al., 2012; Martínez-Vilalta et al., 2009; Pritzkow et al., 2020). For example, sensitivity to VPD_l can be higher in drought-exposed populations of a species compared with those in cooler, more humid environments (Maherali and DeLucia, 2001; Poyatos et al., 2007). Further, recent studies have revealed that numerous hydraulic traits controlling plant responses to supply- and demand-driven water stress show significant plasticity in response to both short-term and long-term environmental conditions such as moisture availability and temperature (Zhang et al., 2020; Feng et al., 2019; Pritzkow et al., 2020).

In addition to controlling fluxes of water and carbon from the plant, g_c also affects canopy temperature, T_c [°C], through the regulation of evaporative cooling, which can be an important mechanism for avoiding thermal stress (Gates, 1968; Lin et al., 2017; Kibler et al., 2023). Evaporation of water from the leaf surface through transpiration (E , [mm hr⁻¹]) reduces leaf and canopy temperatures, which in turn have strong, nonlinear impacts on the rates of photosynthesis and respiration (Berry and Bjorkman, 1980; Way and Yamori, 2014; Yamori et al., 2014; Heskel et al., 2016). Leaf—and, by extension, canopy—temperature is increasingly recognized as an important variable related to plant and ecosystem function due to the negative impacts on photosynthesis when leaf temperatures exceed critical thresholds (~45 °C; Heskel et al., 2016; Slot and Winter, 2017). The canopy thermal response can be quantified by the rate at which canopies warm with air temperature, T_a [°C]; i.e., $\frac{dT_c}{dT_a}$. Historically, observations of well-watered plants have indicated that leaves can cool below air temperature when T_a is very high (i.e., $\frac{dT_c}{dT_a} < 1$; Linacre, 1964; Mahan and Upchurch, 1988), but the extent to which this occurs in natural settings is unclear (Cook et al., 2021; Drake et al., 2020; Blonder and Michaletz, 2018; Yi et al., 2020). Recent canopy-scale evidence across a range of ecosystems suggests that canopy cooling below air temperature does not occur widely, but rather the rate of canopy warming $\frac{dT_c}{dT_a}$ is above one under most natural conditions (Still et al., 2022; Guo et al., 2023; Gauthey et al., 2024; Fig. 1b). As global warming pushes canopy temperatures toward or above critical thresholds (Doughty et al., 2023; Doughty and Goulden, 2008; Slot and Winter, 2017; Mau et al., 2018; Pau et al., 2018), understanding how plants regulate their temperatures, particularly when water is limited, is becoming increasingly important (Urban et al., 2017; Michaletz et al., 2016).

The interacting effects of water limitation, atmospheric moisture demand, and temperature on plant function are difficult to untangle due to a lack of observations across varying conditions. Water limitation, high VPD, and high temperatures often co-occur in natural environments (Dai, 2013; Williams et al., 2013; Seneviratne et al., 2010), making it difficult to isolate their independent effects on plant stress. Studies comparing the relative importance of water supply and atmospheric demand for plant water use and productivity are dominated by comparisons between low demand, high supply (i.e., cool, wet) and high demand, low supply (i.e., hot, dry) conditions (Allen et al., 2015; Cochard, 2021; Grossiord et al., 2018; Anderegg and Meinzer, 2015; Eamus et al., 2013; Fontes et al., 2018). However, these studies lack observations when both supply and demand are either low (cool, dry) or high (hot, wet) (Liu et al., 2020a; Zhou et al., 2019). Furthermore, simultaneous measurements of canopy temperature and mass and energy fluxes are rare, particularly those with accompanying meteorological data (Still et al., 2022).

From a mathematical perspective, regulation of canopy temperature and regulation of water use should be inherently coupled. Transpiration

reduces leaf temperature by helping dissipate the heat absorbed due to incident solar radiation; when stomata close to prevent excess water loss, the subsequent decline in transpiration causes an increase in leaf and canopy temperature. This represents an inherent tradeoff between regulation of water use and canopy temperature: as hydraulic regulation (m) increases (and, by definition, g_c decreases), the rate of canopy warming with air temperature ($\frac{dT_c}{dT_a}$) would be expected to rise, indicating weaker temperature regulation due to a decline in evaporative cooling (Fig. 1c). Conversely, weaker hydraulic regulation ($\downarrow m$) would be associated with stronger regulation of temperature ($\downarrow \frac{dT_c}{dT_a}$), all else being equal, due to a smaller decline in g_c with VPD_l. In either case, water and temperature regulation would be mechanically coupled, with a negative feedback between how tightly water use is controlled and the ability of the plant to regulate its temperature. Hypothetically, m and $\frac{dT_c}{dT_a}$ could become decoupled if $g_{c,\text{ref}}$ is high enough to maintain relatively high conductance as VPD_l and T_a increase. This scenario would require both (1) enough plant-available moisture to allow for continued evaporative cooling under elevated VPD_l (i.e., high supply) and (2) sufficiently high T_a and atmospheric demand to prioritize such cooling (i.e., high demand). Thus, while coupling of water and temperature regulation would be predicted when either water supply or demand are low, decoupling could occur when both supply and demand are high. Consequently, the extent of the water–temperature regulation tradeoff, represented by the steepness of the slopes in Fig. 1c, is an integrated measure of supply- and demand-driven plant behavior that describes a plant's ability to co-regulate water and energy.

Here, we apply this co-regulation framework to observations of canopy conductance, transpiration, and temperature under fluctuating supply and demand conditions to evaluate the relationships between water and temperature regulation in individual plants. We focus on two woody species growing along a large ephemeral river in the Namib Desert, where contrasting seasonal and spatial differences in water availability, VPD, and temperature provide a natural factorial experiment to observe extremes of water and temperature stress (Fig. 2). Using a unique dataset of remotely sensed retrievals of canopy temperature, conductance, and transpiration rates, we first assess species-specific responses of g_c and E to supply- and demand-driven water stress. We then characterize thermal behavior by examining the rate of canopy warming with air temperature as water availability and atmospheric demand fluctuate. Finally, we evaluate the tradeoffs between water and temperature regulation in these desert species by comparing the sensitivity of g_c to VPD_l (m) to the rate of canopy warming with air temperature ($\frac{dT_c}{dT_a}$).

2. Methods

2.1. Study area

The study was conducted at three riparian forest sites along the ephemeral Kuiseb River, a 560-km-long, seasonally flowing river in the central Namib Desert, Namibia (Fig. 2c). Seasonal floods generated from summertime rainfall in the headwaters of the catchment recharge the aquifer in the lower reaches of the Kuiseb (within ~150 km of the coast), supporting a dense gallery forest despite local average rainfall of less than 50 mm yr⁻¹ (Huntley, 1985; Seely et al., 1981). In contrast with more humid systems, trees in the Kuiseb predominantly rely on groundwater and deep soil moisture (Schachtschneider and February, 2010), because the riverbed and shallow soil of the riparian zone are dry nearly year-round; thus, flood frequency and magnitude – rather than soil moisture – are the primary controls on plant-available moisture (Grodek et al., 2020; Jacobson et al., 2000; Seely et al., 1981). As is typical of desert rivers, the Kuiseb is a hydrologically losing system (i.e., discharge decreases downstream), creating a strong gradient of water availability, which decreases from upstream to downstream (Arnold et al., 2016; Grodek et al., 2020; Lange, 2005). When floods do occur sporadically during the summer wet season (Nov–Apr),

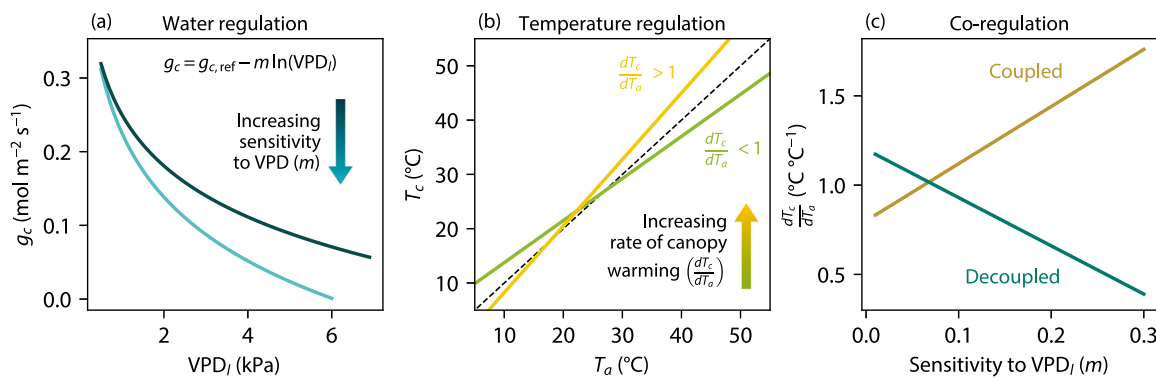


Fig. 1. Conceptual representation of (a) the sensitivity of canopy conductance (g_c) to VPD_l , (b) canopy temperature T_c response to increasing air temperature T_a , and (c) co-regulation of water use (m) and temperature ($\frac{dT_c}{dT_a}$). (a) Canopy conductance is regulated by the maximum g_c at low VPD_l ($g_{c,ref}$) and the sensitivity to VPD_l (m ; Oren et al., 1999). Both m and $g_{c,ref}$ depend on water availability and species-specific hydraulic strategies. (b) The thermal response of the canopy is characterized by the rate at which T_c increases with T_a ($\frac{dT_c}{dT_a}$). A faster rate of warming ($\frac{dT_c}{dT_a} > 1$) results in $T_c > T_a$, while a slower rate of warming ($\frac{dT_c}{dT_a} < 1$) is typically associated with $T_c < T_a$. (c) When water and temperature regulation are coupled, $\frac{dT_c}{dT_a}$ increases with m , indicating a negative feedback between g_c and T_c . Hypothetically, they may become decoupled if supply and demand are high enough, indicated by a negative slope between m and $\frac{dT_c}{dT_a}$.

they typically run dry around 120 km upstream (Arnold et al., 2009). As a result, more frequent flooding in the middle reaches (~105–150 km upstream) results in estimated groundwater recharge rates of ~8.0 $Mm^3 \text{ yr}^{-1}$, more than double the ~2.9 $Mm^3 \text{ yr}^{-1}$ recharged to the aquifer farther downstream (~70–105 km from the coast; Grodek et al., 2020; Dahan et al., 2008). Silt content also peaks in the middle reaches, allowing soils to retain moisture for longer after flooding compared to the sandy downstream channel and floodplains (Jacobson et al., 2000). Data were collected at three sites (Fig. 2c): one in the wetter reaches (15.2942° E, -23.6666° S; 140 km upstream) and two in the dry lower reaches (15.0315° E, -23.5569° S and 14.8702° E, -23.3601° S; 104 and 74 km upstream, respectively). While groundwater levels during the study period were not available, long-term flood records indicate that while nearly all flood events reach the upstream site, over half run dry before reaching the downstream sites (Fig. 2d; Grodek et al., 2020; Morin et al., 2009; data from the Ministry of Agriculture, Water and Forestry, Department of Water Affairs, Hydrology Division, Windhoek, Namibia). Higher water availability in this upstream reach has been linked to higher tree density (Morgan et al., 2020; Theron et al., 1980) and fluctuations in long-term forest productivity (Morgan et al., 2021; Grodek et al., 2020).

As a coastal desert, the Namib experiences mean annual temperatures around 22 °C, with an average diurnal temperature range of 9–27 °C during the coolest three months of the year (Jul–Sep) and 16–33 °C during the hottest months (Mar–May; Southern African Science Service Centre for Climate Change and Adaptive Land Management WeatherNet, 2023; Fig. 2b). Data were collected in two campaigns, one at the end of the hot, wet season (10–14 May 2022) and one in the cool, dry season (22–26 Sep 2022). Hot season flights were timed to capture peak T_a and VPD_a , which occurs between Apr and May, so as to maximize the difference in demand and heat stress and minimize the difference in water availability between the two seasons (Table 1). We thus assume water availability is roughly constant between the two seasons and use the sites to distinguish high and low plant-available moisture conditions (Fig. 2a).

We focused on the two dominant tree species in the lower Kuiseb ecosystem: *Acacia* (*Vachellia*) *erioloba* and *Faidherbia* *albida*. Though the leaves and canopies are structurally similar, the two species differ in their physiological traits and growth patterns (Coates Palgrave, 2002). With higher wood density, smaller xylem vessels, and lower xylem water potentials (Schachtschneider, 2010; Barnes et al., 1997; Timberlake et al., 1999), *A. erioloba* is more drought-tolerant than *F. albida*, which is more susceptible to water stress (Ward and Breen, 1983; Theron et al., 1985; Rouspard et al., 1999). While both species

are very deeply rooted, with reported rooting depths in excess of 30 m in some areas (Dupuy and Dreyfus, 1992; Canadell et al., 1996), *F. albida*, a facultative phreatophyte, is typically restricted to growing near the active channel, where the water table is shallower. In contrast, *A. erioloba* has a wider distribution, including on the fringes of the riparian zone where the water table is deeper (Morgan et al., 2020; Seely et al., 1981).

2.2. Approach for retrieving canopy temperature and transpiration

Thermal remote sensing allows for retrieval of surface temperature information across large areas, providing an efficient way to characterize landscape-scale evapotranspiration (Zhang et al., 2016; Kustas and Anderson, 2009). Unmanned aerial vehicles (UAVs) equipped with thermal sensors can capture thermal data at centimeter-scale resolution, which enables retrievals of canopy temperature and transpiration at the scale of individual plant canopies (McCabe et al., 2017; Berni et al., 2009). We used UAV-based retrievals of T_c and meteorological data to calculate plant-scale transpiration with a novel surface energy balance algorithm (Morgan and Caylor, 2023). The approach enables retrieval of transpiration rates with the same precision as eddy covariance measurements at very-fine- (centimeter-) scales solely using data obtained from a UAV platform, allowing us to constrain organismal-level responses to water and heat stress.

The full details of the platform, data processing workflow, and algorithm used for calculations are described in Morgan and Caylor (2023), and details specific to this study can be found in the Supporting Information. In brief, the UAV platform consisted of a DJI Matrice 600 Pro hexacopter UAV equipped with a radiometrically calibrated multispectral and thermal infrared sensor (MicaSense Altum, MicaSense Solutions, Seattle, WA, USA), a high-precision global navigation satellite system (GNSS) module (Emlid Reach M2, Emlid, Budapest, Hungary) for georeferencing, two pyranometers (LI-200R, LI-COR Biosciences, Lincoln, NE, USA) to measure incoming and outgoing shortwave radiation, and an ultrasonic anemometer and weather sensor (TriSonica Mini Wind and Weather Sensor, LI-COR Biosciences, Lincoln, NE, USA) for collecting meteorological data. In addition to shortwave radiation, meteorological data included air temperature, relative humidity, air pressure, and wind speed and were collected at 5 Hz for the duration of the flight and for 5 to 10 min on the ground (1.5 m) before and after each flight. The 1.5-m meteorological data were used for analysis of site conditions and subsequent calculations as these were closest to canopy-level conditions.

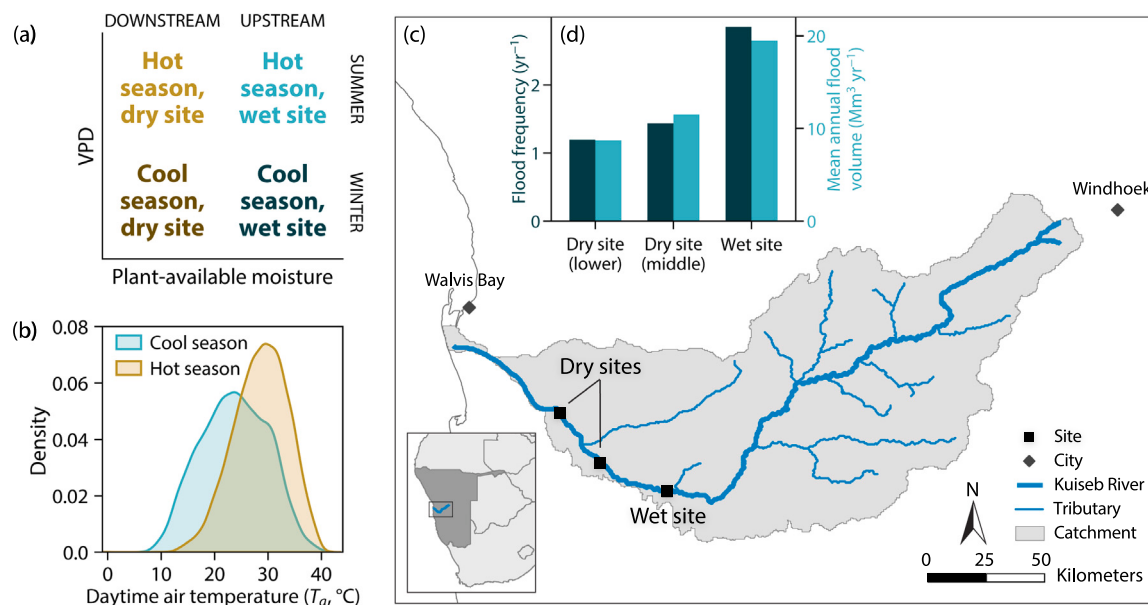


Fig. 2. Climatology and hydrology of the Kuiseb River catchment. (a) Observational framework showing the four scenarios of relative supply (plant-available moisture) and demand (VPD). (b) Distribution of daytime air temperatures by season. Kernel density estimates show hourly daytime (8:00–20:00) air temperatures during the hottest (Mar–May) and coolest (Jul–Sep) three months of the year. Data for the Gobabeb meteorological station (located at the dry middle site) were obtained for 2015–2022 from the Southern African Science Service Centre for Climate Change and Adaptive Land Management WeatherNet (2023). (c) The Kuiseb catchment, including the three study sites. Moisture availability decreases downstream (roughly east to west). We included one site in the middle reaches of the river within the Kuiseb Canyon and two in the lower, drier reaches. (d) Flood magnitude and frequency at each of the study sites, derived from modeled flows in Grodek et al. (2020) and data from the Ministry of Agriculture, Water, and Forestry of Namibia for floods between 1960 and 2006.

During each of the two seasonal campaigns, we conducted five diurnal flights at each site in approximately 90-minute intervals between 9:00 and 15:30 local time on 1–2 days each season. Flights were conducted at an altitude of 75 m and lasted an average of 18.3 min. All data for a given season were collected within five days to ensure similar conditions at each site, and diurnal sampling times were consistent across sites and seasons. In total, we analyzed data across 20 wet season and 17 dry season flights.

The raw, 6-band images (visible, near-infrared, thermal infrared) from each flight were mosaicked to produce a single orthoimage for each flight, and in-flight meteorological data were used to perform atmospheric corrections and convert thermal infrared data from brightness values to surface temperature. The spatial resolution of resulting surface temperature orthoimages was approximately 40–50 cm. We calculated net radiation (R_n [W m^{-2}]), sensible heat flux, and latent heat flux (λE [W m^{-2}]), the energy equivalent of evapotranspiration, from the thermal imagery, using the aeroet package (Morgan, 2023) in Python (see Supporting Information for details). We used normalized difference vegetation index (NDVI) information from the UAV images to exclude non-vegetated pixels; thus, our estimates of λE consist only of plant transpiration, calculated from λE by dividing by the latent heat of vaporization, λ [J kg^{-1}] and converting instantaneous values (mm s^{-1}) into hourly estimates (mm hr^{-1}). Individual tree canopy values of T_c and E were extracted as described in Section 2.3 and used for subsequent calculation of g_c and VPD_l (Section 2.4).

2.3. Tree surveys

To supplement the data acquired by the UAV system, we conducted field surveys of tree locations and structure. At each site, we surveyed between 80 and 166 individuals, chosen randomly. For each individual, we recorded the species, diameter-at-breast height (DBH), trunk locations, and crown perimeters (See Section S3). Location and crown perimeters were mapped using a high-precision global navigation satellite system (GNSS) unit (Reach RS2, Emlid, Budapest, Hungary).

Table 1

Environmental conditions during the two campaigns. Maximum observed T_a and VPD_a were acquired from UAV-mounted sensors at a height of 1.5 m before and after each flight. Mean daytime (8:00–18:00) conditions were calculated from the Gobabeb meteorological station located near the dry middle site (Southern African Science Service Centre for Climate Change and Adaptive Land Management WeatherNet, 2023). Conditions during each season were similar between the dry and wet sites.

		Maximum observed	Mean daytime (8:00–18:00)
Hot season	T_a	32.47 °C	30.12 °C
	VPD_a	3.93 kPa	3.7 kPa
Cool season	T_a	27.39 °C	22.26 °C
	VPD_a	2.17 kPa	1.95 kPa

The post-processing workflow for the GNSS data involved Precise Point Positioning using Natural Resources Canada's Canadian Geodetic Survey website (Natural Resources Canada Canadian Geodetic Survey, 2022) to correct the position of the base module, followed by post-processing kinematics analysis of the rover logs in Emlid Studio 1.5 (Emlid, Budapest, Hungary). Surveyed points were aligned with the corrected logs based on their timestamps.

A polygon for each tree crown was created from the convex hull of the corresponding survey points and used to extract minimum, maximum, and mean values of T_c and E for each individual tree from the processed images. For overlapping tree crowns, the canopy height models were used to assign pixels to the tallest tree. The workflow for deriving canopy height is described in Section S2.

2.4. Calculation of canopy conductance, g_c

To calculate canopy conductance, we inverted the flux-gradient equation for latent heat to first derive canopy resistance, r_c [s m^{-1}]:

$$r_c = \lambda_v \rho_a \frac{q_c - q_a}{\lambda E} - r_H, \quad (1)$$

where λ_v is the latent heat of vaporization [J kg^{-1}], ρ_a [kg m^{-3}] is the density of air, q_c and q_a [kg kg^{-1}] are the specific humidities of the canopy and the air, respectively, and r_H [s m^{-1}] is the resistance to heat and vapor transport. Canopy conductance, g_c [m s^{-1}], is the inverse of this value, $g_c = 1/r_c$, and can be converted to molar units [$\text{mol m}^{-2} \text{s}^{-1}$], more commonly used in physiological studies, using the ideal gas law.

This approach is analogous to those commonly used to calculate surface conductance by inverting the Penman–Monteith equation (Penman, 1948; Monteith, 1965). In this case, q_c can be directly calculated from T_c , assuming the canopy vapor pressure is at saturation, making Eq. (1) more accurate than using the Penman–Monteith linearization. Aerodynamic resistance, r_H , is calculated iteratively from sensible heat flux, starting with an initial assumption of a neutral atmosphere and solving until convergence between calculations is reached (see Supporting Information for details).

2.5. Analysis of water and temperature regulation

To evaluate plant water regulation, we compared the sensitivity of g_c and E to VPD_l across the four observation conditions (Fig. 2a). First, we fit retrievals of g_c at the individual and site scales to the following equation that describes the relationship between g_c and VPD_l (Oren et al., 1999):

$$g_c = g_{c,\text{ref}} - m \ln(\text{VPD}_l), \quad (2)$$

where the reference conductance, $g_{c,\text{ref}}$, is the canopy conductance at reference VPD_l (usually 1 kPa) and m describes the sensitivity of g_c to VPD_l , as discussed in Section 1. A plant that is more sensitive to VPD_l would have a higher m . Although VPD_l more accurately represents the actual gradient that drives the moisture flux from the plant canopy, atmospheric VPD , VPD_a , is often substituted for VPD_l in Eq. (2) because VPD_l requires canopy temperature information, which is not always available. Here, we use T_c to calculate VPD_l for each individual tree canopy:

$$\text{VPD}_l = e^*(T_c) - e(T_a) \quad (3)$$

where $e(T)$ is the vapor pressure [kPa] at temperature T . The vapor pressure of the canopy is assumed to be at saturation, denoted e^* . We used diurnal observations of g_c and VPD_l to fit Eq. (2) and compare m and $g_{c,\text{ref}}$ across seasonal changes in VPD_a and T_a , as well as spatial differences in water availability.

In addition to conductance, we evaluated the relationship between E and VPD_l in order to explore the extent to which sensitivity in g_c affects transpiration under different supply and demand conditions. Transpiration rates were fit with second-order polynomials (Grossiord et al., 2020; Monteith, 1995), to estimate the peak rate (E_{\max} , [mm hr^{-1}]) under each of the four scenarios.

To characterize temperature regulation, we derived the slopes $\frac{dT_c}{dT_a}$ by regressing T_c on T_a . Mean values of T_c and E across each canopy were used to calculate g_c and VPD_l and in all analyses.

We derived metrics m , $g_{c,\text{ref}}$, and $\frac{dT_c}{dT_a}$ for each set of conditions – hot, wet; cool, wet; hot, dry; cool, dry – and for the individual trees under the same four scenarios. We compared individual-scale m and $\frac{dT_c}{dT_a}$ to evaluate the relationship between water and temperature regulation across the four scenarios using linear regression to identify the direction and strength of co-regulation.

Data were filtered to omit VPD_l outliers ($\text{VPD}_l > 8 \text{ kPa}$), non-transpiring trees (maximum $E < 0 \text{ mm hr}^{-1}$) and low radiation conditions ($R_n < 100 \text{ W m}^{-2}$), except in the case of E , for which low radiation data were not excluded, as the equation requires low E and VPD_l values for a proper fit. As a result, we analyzed 2,127 observations of 306 individual trees. For the individual data, trees with too few observations or invalid coefficients (i.e., $g_{c,\text{ref}} < 0$) were omitted, so results for 267 trees were included in the subsequent analysis.

All analyses were performed in Python 3.10.

3. Results

The tree species had different responses to supply- and demand-driven water stress, but similar responses to thermal stress. Under most conditions, they experienced tradeoffs between hydraulic function and avoiding thermal stress, but when both supply and demand were high, regulation of water use and canopy temperature were decoupled.

3.1. Regulation of water use

The two species had different maximum transpiration rates and showed contrasting responses to changes in water supply and atmospheric demand (Fig. 3). Under unstressed (cool, wet) conditions, *F. albida* trees had higher estimated reference conductance and peak transpiration rates ($g_{c,\text{ref}} = 0.166 \text{ mol m}^{-2} \text{s}^{-1}$, $m = 0.084$, $r^2 = 0.37$, $p < 0.001$; $E_{\max} = 0.117 \text{ mm hr}^{-1}$) than *A. erioloba* ($g_{c,\text{ref}} = 0.078 \text{ mol m}^{-2} \text{s}^{-1}$, $m = 0.039$, $r^2 = 0.47$, $p < 0.001$; $E_{\max} = 0.083 \text{ mm hr}^{-1}$). When demand and T_a were higher, both species had slightly increased reference conductances (*A. erioloba*: $g_{c,\text{ref}} = 0.099 \text{ mol m}^{-2} \text{s}^{-1}$, $r^2 = 0.38$, $p < 0.001$; *F. albida*: $g_{c,\text{ref}} = 0.199 \text{ mol m}^{-2} \text{s}^{-1}$), and *F. albida* was more sensitive to VPD_l ($m = 0.106$, $r^2 = 0.48$, $p < 0.001$).

When water availability was lower, however, *A. erioloba* showed a slight decline in both g_c and transpiration under cool conditions ($g_{c,\text{ref}} = 0.037 \text{ mol m}^{-2} \text{s}^{-1}$, $r^2 = 0.40$, $p < 0.001$; $E_{\max} = 0.035 \text{ mm hr}^{-1}$), but sustained g_c and transpiration near well-watered rates when demand and air temperature were high ($g_{c,\text{ref}} = 0.051 \text{ mol m}^{-2} \text{s}^{-1}$, $r^2 = 0.42$, $p < 0.001$; $E_{\max} = 0.071 \text{ mm hr}^{-1}$).

Dry conditions led to higher VPD_l sensitivity of *F. albida* ($m = 0.087 \text{ mol m}^{-2} \text{s}^{-1}$, $r^2 = 0.44$, $p < 0.001$), but no significant change in $g_{c,\text{ref}}$ ($0.131 \text{ mol m}^{-2} \text{s}^{-1}$). Under hot, dry conditions, *F. albida* individuals downregulated conductance ($g_{c,\text{ref}} = 0.103 \text{ mol m}^{-2} \text{s}^{-1}$), but the sensitivity to VPD_l was only slightly reduced relative to unstressed conditions ($m = 0.054$, $r^2 = 0.40$, $p < 0.001$). Peak transpiration rates declined when water availability was lower in both hot ($E_{\max} = 0.068 \text{ mm hr}^{-1}$) and cool ($E_{\max} = 0.062 \text{ mm hr}^{-1}$) conditions.

Responses of conductance and transpiration to VPD_l were similar across sites and individuals, with a few minor differences (see Section S5 for details). Canopy conductance of both species showed a logarithmic relationship to VPD_l under all conditions.

3.2. Regulation of canopy temperature

The relationships between canopy temperature and air temperature are shown in Fig. 4. In the cool season, canopies warmed faster than the air under both wet ($\frac{dT_c}{dT_a} = 1.16 \text{ }^{\circ}\text{C }^{\circ}\text{C}^{-1}$, $r^2 = 0.66$, $p < 0.001$) and dry ($\frac{dT_c}{dT_a} = 1.07 \text{ }^{\circ}\text{C }^{\circ}\text{C}^{-1}$, $r^2 = 0.69$, $p < 0.001$) conditions, with no significant differences between the species. When temperatures are higher during the hot season, however, canopies showed slower rates of warming than the air, causing the canopy-to-air temperature difference ($T_c - T_a$) to decrease with increasing air temperature, leading to $\frac{dT_c}{dT_a}$ slopes of $0.82 \text{ }^{\circ}\text{C }^{\circ}\text{C}^{-1}$ ($r^2 = 0.60$, $p < 0.001$) and $0.87 \text{ }^{\circ}\text{C }^{\circ}\text{C}^{-1}$ ($r^2 = 0.70$, $p < 0.001$) under wet and dry conditions, respectively (Fig. 4). The two species showed slightly different responses under these conditions, with a significant decrease in $\frac{dT_c}{dT_a}$ under hot, dry conditions only for *F. albida* (Fig. S6). These were the only conditions under which the two species' slopes differed significantly.

Despite having slopes of less than 1, canopies were still much warmer than the air in the wet season, even at high T_a due to their higher temperatures under cooler morning conditions (represented by higher intercepts in Fig. 4b). *A. erioloba* was warmer than *F. albida* under nearly all conditions, but the two species consistently showed similar warming rates as a function of air temperature (Table S3).

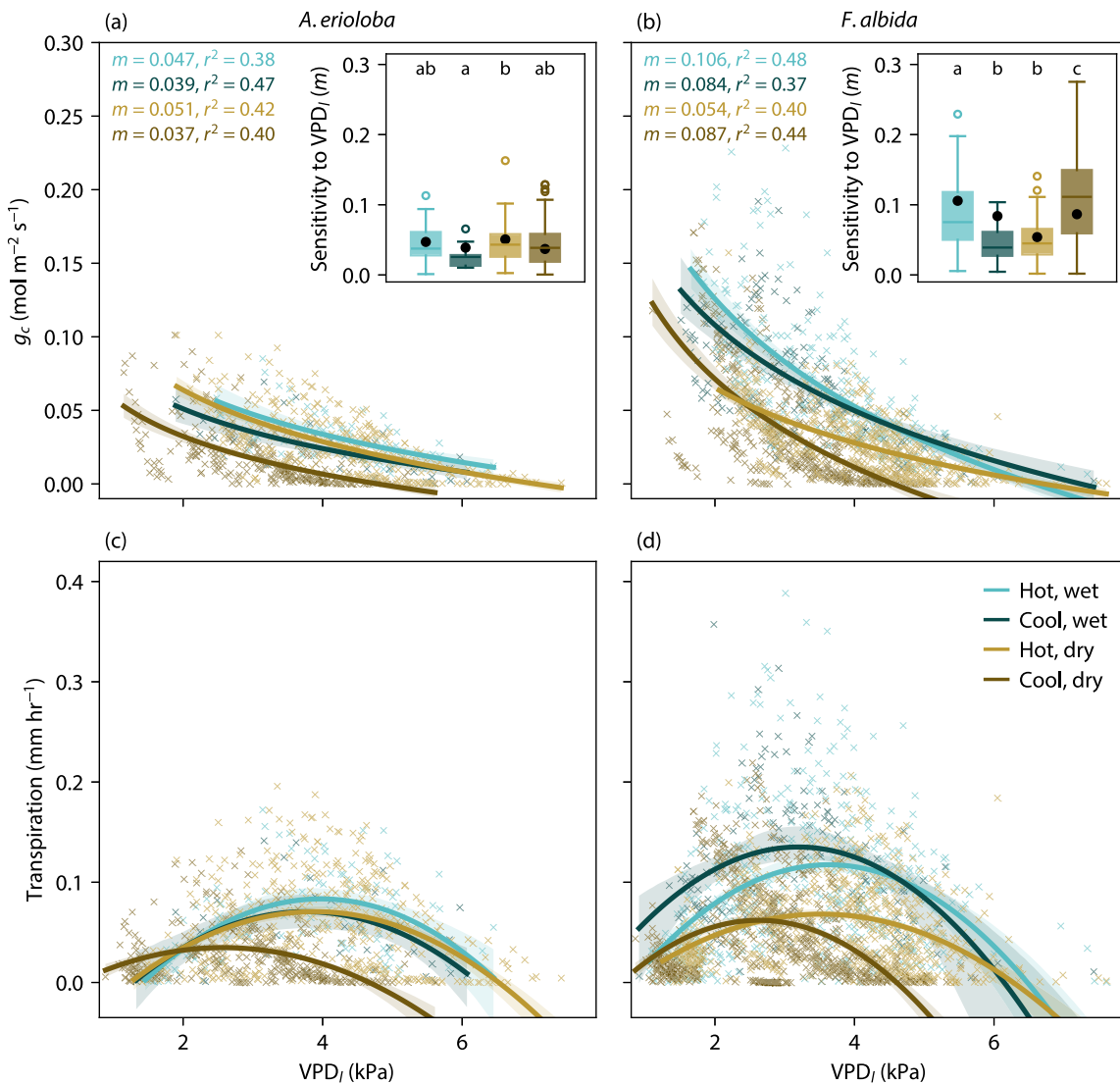


Fig. 3. Sensitivity of canopy conductance (a, b) and transpiration (c, d) to VPD_I of each species for the four scenarios. Individual-tree observations are shown ("x") with regression lines fitted to all data for a given scenario. Conductances were fitted with a logarithmic relationship (Eq. (2); Oren et al., 1999), and transpiration rates were fitted with a second-order polynomial (Grossiord et al., 2020). Shaded regions denote the 95% confidence interval of the regression estimates. Insets in (a) and (b) show sensitivities of individual trees. Box plots show the medians and the interquartile range; whiskers extend 1.5 times the interquartile range from each box. The black points denote the site-level coefficients corresponding to the curves in each plot. Letters denote statistically significant differences between median values (Kruskal-Wallis test $p < 0.05$) where groups that do not contain the same letter are different.

3.3. Tradeoffs between water and temperature regulation

Under cool conditions, the relationship between m and $\frac{dT_c}{dT_a}$ was positive (wet: $1.63, r^2 = 0.09, p = 0.05$; dry: $1.11, r^2 = 0.05, p = 0.001$), indicating a tradeoff between water and temperature regulation (Fig. 5). In both cool, wet and cool, dry conditions, the intercepts were slightly greater than 1 (wet: $1.04 \text{ }^\circ\text{C }^\circ\text{C}^{-1}$, dry: $1.08 \text{ }^\circ\text{C }^\circ\text{C}^{-1}$), which indicates that canopies warm faster than the air even when the sensitivity to VPD_I is low. The relationship between m and $\frac{dT_c}{dT_a}$ is also positive under hot, dry conditions, with a steeper slope ($3.93, r^2 = 0.14, p < 0.001$) indicating stronger tradeoffs between water use and temperature regulation than when temperatures are cooler. The intercept was lower ($0.82 \text{ }^\circ\text{C }^\circ\text{C}^{-1}$), suggesting that canopy cooling occurs when VPD_I sensitivity is low. When both supply and demand were high (hot, wet conditions), the relationship between m and $\frac{dT_c}{dT_a}$ was negative ($-0.88, r^2 = 0.05, p = 0.08$), indicating that as sensitivity to VPD_I increased, temperature regulation increased. These patterns were consistent across species, with some differences in the magnitude of the coefficients (Fig. S7).

4. Discussion

While regulation of water use differs between species and in response to changes in water supply and demand, temperature regulation shows sensitivity only to seasonal variations in air temperature and atmospheric demand. These patterns lead to variation in the coupling between water and temperature regulation in response to changing water supply and atmospheric demand and reveal two important mechanisms for withstanding stressful conditions: (1) upregulation of g_c in *F. albida* under cool, dry conditions and (2) decoupling of water and temperature regulation under hot, wet conditions.

Contrasts in water regulation between species and in response to changes in supply and demand reflect the nuanced, species-specific strategies that *F. albida* and *A. erioloba* have adopted to navigate the confluence of water and thermal stress in hyperarid landscapes. Under relatively unstressed (cool, wet) conditions, *F. albida* has higher reference conductance and peak transpiration rates than *A. erioloba*, consistent with both previous findings (Bate and Walker, 1993) and the likelihood that *F. albida* has greater access to water due to its proximity

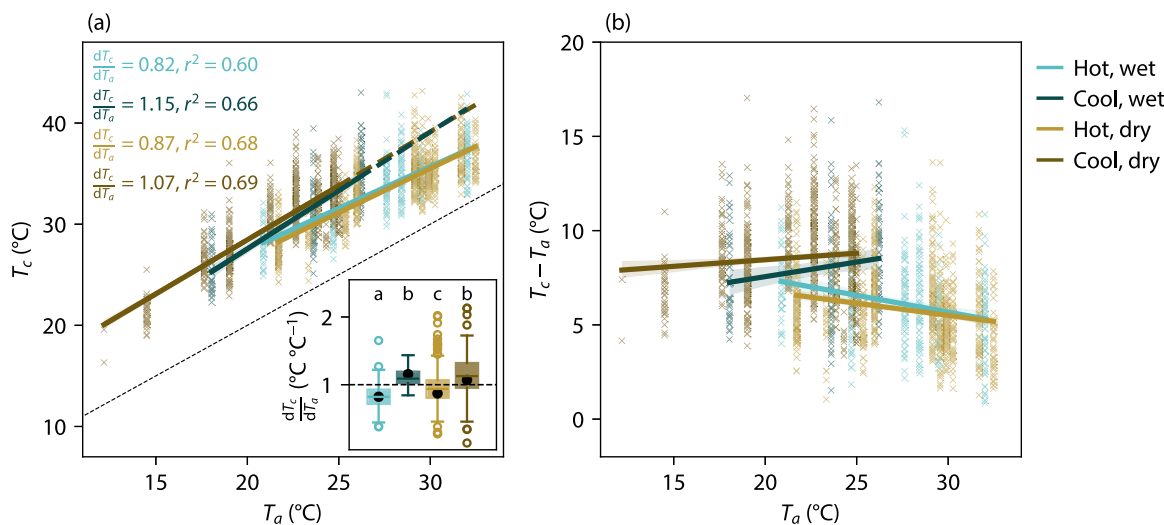


Fig. 4. Relationships between (a) canopy temperature T_c and (b) the difference between canopy and air temperatures and air temperature T_a for the four scenarios. Individual-tree observations are shown ("x") with regression lines fitted to all data for a given scenario; shaded regions indicate the 95% confidence interval. Slopes in (a) represent the increase T_c with T_a , i.e., $\frac{dT_c}{dT_a}$. In (b), the y-axis represents the instantaneous temperature difference between the canopy temperature and air temperature, where the slope is $\frac{dT_c}{dT_a} - 1$ and the intercept is the difference between canopy and air temperatures under cooler conditions (usually early morning). Slopes of $\frac{dT_c}{dT_a}$ were fairly consistent across scales and between species (Fig. S6). The inset in (a) shows the sensitivity of T_c to T_a of individual trees. Box plots show the medians and the interquartile range; whiskers extend 1.5 times the interquartile range from each box. The black points denote the site-level coefficients corresponding to the slopes of the lines in (a). Letters denote statistically significant differences between median values (Kruskal–Wallis test $p < 0.05$) where groups that do not contain the same letter are different.

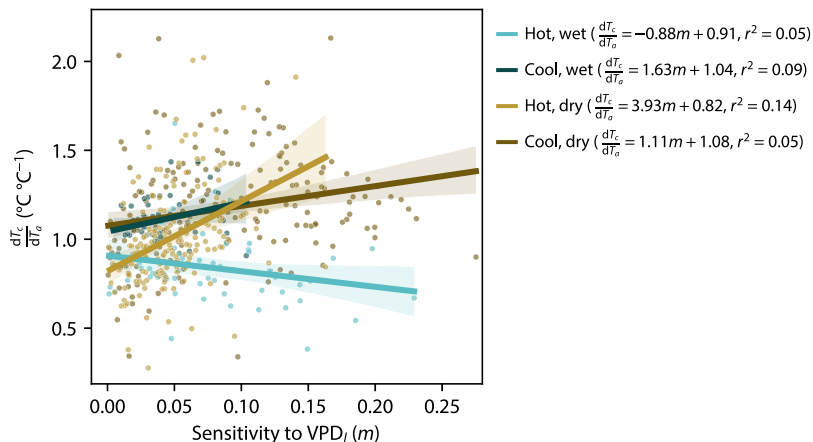


Fig. 5. Co-regulation of water and temperature. Points denote the sensitivities of conductance (m) and temperature ($\frac{dT_c}{dT_a}$) of individual trees. Regression lines show the relationship between regulation of water use and regulation of temperature with shaded regions denoting the 95% confidence interval. Relationships were similar across the two species (Fig. S7).

to the channel (Morgan et al., 2020; Seely et al., 1981). In addition, the two species diverge in their responses to dry conditions. When water availability is lower, *A. erioloba* maintains g_c and transpiration near well-watered rates when demand and air temperature are high. This persistence of high g_c values reflects more profligate, anisohydric water-use behavior, in which high transpiration rates continue, even as water availability declines. *F. albida*, on the other hand, strongly downregulates g_c when supply is low and demand is high, leading to a decrease in transpiration. These divergent responses indicate that anisohydric behavior may increase sensitivity to demand when supply is low, while isohydricity may be associated with greater sensitivity to supply when atmospheric demand is high. This is consistent with other studies showing that across biomes, more conservative, isohydric species tend to have higher reference conductance ($g_{c,\text{ref}}$, $[\text{mol m}^{-2} \text{s}^{-1}]$), but may be more sensitive to VPD_l than more profligate species (Cunningham, 2004; Berger-Landefeldt, 1936). Importantly, these strategies can be

important for species' drought responses; rates of dieback and mortality during drought periods are much lower in *A. erioloba* than *F. albida* (Ward and Breen, 1983; Theron et al., 1985), similar to other anisohydric species that are more drought-resilient than co-occurring isohydric species (McDowell et al., 2008).

Our observational framework extends the analysis of species' responses beyond commonly occurring hot, dry conditions into less frequently observed cool, dry conditions. Importantly, we find that *F. albida* increases conductance under cooler, more humid conditions, even when water availability is low, suggesting active stomatal acclimation to changes in VPD and temperature. When water is limiting, *F. albida* increases g_c under cool, humid conditions and reduces g_c when T_a and VPD are high, as illustrated in Fig. 1a. The depressed g_c under hot, dry conditions is similar to findings in isohydric species, such as piñon pine (*Pinus edulis*; Grossiord et al., 2017). However, the increase in g_c under cool, water-limited conditions is surprising

in this water-demanding species. Importantly, the cool, humid atmosphere suppresses transpiration despite high conductance (Fig. 3b,d), enabling higher rates of photosynthesis without excess water loss. This is likely a key productivity window for this species and could explain its characteristic reverse phenological cycle, which leads to the production of pods and flowers in the cooler dry season (Roupsard et al., 1999). However, the sensitivity to elevated VPD_a and T_a in the summertime suggests that more conservative species like *F. albida* could be particularly vulnerable to increased temperatures and VPD due to global warming, even if water availability remains constant, as higher temperatures reduce g_c and thus carbon acquisition.

While hydraulic regulation varies between the species, their behavior with regard to temperature regulation is similar and largely dependent on environmental conditions. In the cool season, $\frac{dT_c}{dT_a}$ is greater than 1 for both species, indicating that, like in most environments, the plant canopies warm faster than the air (Still et al., 2022). These findings confirm recent theoretical (Blonder and Michaletz, 2018) and empirical (Still et al., 2022) evidence that megathermy ($\frac{dT_c}{dT_a} > 1$) dominates under most natural conditions, particularly when water is limiting. However, the low summertime slopes provide evidence that temperature regulation in desert canopies can shift seasonally in response to higher air temperatures, leading to canopies warming more slowly than the air ($\frac{dT_c}{dT_a} < 1$). Importantly, though, canopy-air temperature relationships in which $\frac{dT_c}{dT_a} < 1$ do not equate to canopies cooling below the air temperature, as is typically assumed. In this case, when $\frac{dT_c}{dT_a} < 1$, cool, early morning canopy temperatures are still several degrees above air temperature, so we never observed canopies cooling below air temperature. In fact, the intercepts in Fig. 4 are such that air temperatures would have to reach unrealistically high values (>90 °C) for T_c to cool below T_a . Nevertheless, regulation of canopy temperature in the hottest time of year such that $\frac{dT_c}{dT_a} < 1$ keeps average daily maximum temperatures within 1 °C of their cool season maxima ($T_{c,max,hot} = 37.5$ °C; $T_{c,max,cool} = 36.6$ °C) despite daytime air temperatures that are 5 °C higher in the hot season than the cool season. Hypothetically, if canopies warmed at the faster (cool season) rate during the hot season, they would reach temperatures of 41.5 °C on average (Fig. 6). Thus, evaporative cooling appears to be an important mechanism for avoiding thermal stress when air temperatures are high.

Under most conditions, desert trees experience a tradeoff between avoiding water stress and avoiding thermal stress. When T_a and atmospheric demand are low, or when water availability is low and when T_c and demand are high, the slope of the relationship between m and $\frac{dT_c}{dT_a}$ is positive: increasing hydraulic regulation ($\uparrow m$) leads to decreasing temperature regulation ($\uparrow \frac{dT_c}{dT_a}$), and vice versa (Fig. 5). In the hot, dry case, trees with lower sensitivity to VPD_l more strongly regulate their temperatures. However, even though evaporative cooling allows $\frac{dT_c}{dT_a} < 1$ for most trees (Fig. 4), water availability is not high enough to meet the elevated atmospheric demand, so the consequence of stomatal closure is a greater increase in $\frac{dT_c}{dT_a}$ than when demand is lower. Thus, under cool or water-stressed conditions, stomatal control prioritizes water regulation over temperature regulation, with coupling between the two increasing as hydraulic regulation increases.

The decoupling of water and temperature regulation under hot, wet conditions, on the other hand, suggests that trees at the wetter upstream site had access to sufficient water resources to maintain evaporative cooling despite higher demand. In this scenario, increased sensitivity of g_c to VPD_l ($\uparrow m$) enhances temperature regulation ($\downarrow \frac{dT_c}{dT_a}$; Fig. 5). While seemingly counterintuitive, this result may be due to an increase in $g_{c,ref}$ which is roughly linearly related to m (Grossiord et al., 2020). These conditions result in an increase in g_c , leading water and temperature regulation to become decoupled. Regardless, the relationship between m and $\frac{dT_c}{dT_a}$ suggests that if water availability is high enough, transpiration and evaporative cooling are sustained at a high rate such that $\frac{dT_c}{dT_a} < 1$ without compromising hydraulic safety. In

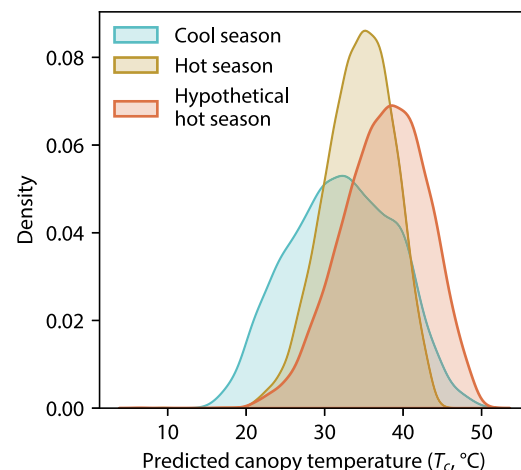


Fig. 6. Modeled seasonal distributions of daytime canopy temperatures. Modeled canopy temperatures are just 2.1 °C higher on average due to lower rates of canopy warming in the hot season (mean daily $T_{c,hot} = 34.4$ °C, $\frac{dT_c}{dT_a} = 0.86$, $r^2 = 0.67$, $p < 0.001$) compared to the cool season (mean daily $T_{c,cool} = 32.3$ °C, $\frac{dT_c}{dT_a} = 1.07$, $r^2 = 0.68$, $p < 0.001$). Hypothetically, if canopies warmed at the faster (cool season) rate during the hot season, when air temperatures are higher, they would reach mean daytime temperatures of 37.6 °C on average, with average daily maximum temperatures of 41.5 °C. Models of T_c were derived by regressing T_c on T_a for all data (i.e., from both sites) by season. Historical hourly daytime T_a data (Fig. 2b) were used to predict daytime T_c for the hottest and coolest three months of the year. The hypothetical hot season curve is derived by applying the cool season equation to historical hot season air temperatures. Curves show kernel density estimates.

other words, trees do not experience a tradeoff between water loss and temperature regulation if both supply and demand are high enough.

The relationships between m and $\frac{dT_c}{dT_a}$ highlight tradeoffs in plants' ability to co-regulate water and energy, providing insight into the combined effects of water and temperature stress on plant behavior. By integrating water availability and atmospheric demand, the slope of this relationship functions as a holistic measure of a plant's capacity to use water to regulate its energy balance. The steeper slope under hot, dry conditions relative to when the atmosphere is cooler and more humid suggests that plants are most stressed when supply is low and demand is high, which is consistent with expected behavior. The more surprising result is that the slope is negative under hot, wet conditions but positive under cool, wet conditions. While this could be due to a seasonal difference in water availability between the wet (hot) and dry (cool) seasons in the study area, the increase in conductance in *F. albida* at the wetter site in the cooler dry season suggests that plant-available moisture remains high enough to sustain year-round transpiration even in a more conservative species. Furthermore, from a co-regulation perspective, the decoupling of water and temperature regulation under hot, wet conditions aligns with what would be expected in an environment like this, where access to the riparian groundwater aquifer facilitates the survival of woody species in an otherwise hyperarid environment.

Our findings under cool, dry and hot, wet conditions reveal two unexpected responses that could be particularly vulnerable to climate-induced water and temperature stress. First, a purely isohydric strategy would suggest that *F. albida* would decrease g_c and transpiration in all water-stressed conditions, but we find that this species upregulates g_c – and photosynthesis – under cooler atmospheric conditions. This is likely an important mechanism for carbon uptake in hyperarid systems for this more drought-sensitive species. Even if water availability does not change in the region in the future, *F. albida* may be vulnerable to increasing winter temperatures, given its sensitivity to hot, dry atmospheric conditions when water resources are less abundant. Increasing

VPD due to rising temperatures is predicted globally (Douville et al., 2022; Sherwood and Fu, 2014; Berg et al., 2016), and recent evidence suggests that relative humidity is declining as well, resulting in an even more substantial increase in VPD than previously predicted (Simpson et al., 2024). These exacerbated VPD increases are particularly strong in drylands (Simpson et al., 2024; Held and Soden, 2006) and could substantially reduce the productivity of desert species in the cool, dry season.

Secondly, we find that water and temperature regulation are decoupled under hot, wet conditions, which emphasizes the importance of evaporative cooling for mitigating thermal stress. While slower rates of canopy warming with air temperature have been observed previously in irrigated plants (Urban et al., 2017; Upchurch and Mahan, 1988), recent meta-analyses have suggested that canopies warm faster than the air (i.e., $\frac{dT_c}{dT_a} > 1$) in nearly all natural environments (Still et al., 2022; Guo et al., 2023). We find that moderately high (~32 °C) maximum daily air temperatures can induce canopy temperature regulation such that $\frac{dT_c}{dT_a} < 1$, so long as plants have relatively stable water access (e.g., in a frequently inundated riparian zone). Modeled canopy temperatures show that this behavior prevents daily maximum canopy temperatures from reaching 40 °C, which they would otherwise exceed over two-thirds of the time during the hottest three months of the year (Fig. 6). Because these months occur at the end of the wet season, higher water availability may contribute to the trees' ability to cool canopies via transpiration. Moreover, observed maximum canopy temperatures exceeded the suggested critical temperature for photosynthetic function (~46.7 °C; Slot et al., 2021) in 47.6% of our observations, with more frequent occurrences in *A. erioloba* and under hot, dry conditions. Even in the wettest conditions, parts of the canopy exceeded this threshold 43.6% of the time. Above this threshold (T_{crit}), which is identified by a drop in chlorophyll fluorescence, the leaf photosystem collapses, ultimately leading to necrosis and death (Krause et al., 2010). Importantly, T_{crit} tends to be higher in species growing in warmer, drier climates (Kitudom et al., 2022; O'Sullivan et al., 2017) and can even change seasonally (Zhu et al., 2018) in response to higher air temperatures, with some observations of T_{crit} as high as 55 °C (Gauthey et al., 2024). Given that we did not observe widespread, anomalous canopy dieback in the Kuiseb species despite high canopy temperatures, T_{crit} in these desert trees is elevated, allowing them to maintain a positive thermal safety margin (that is, $T_c < T_{crit}$). Nonetheless, most species reach a photosynthetic optimum at leaf temperatures well below 40 °C (Medlyn et al., 2002), and high temperatures are associated with a decline in various other physiological processes (Heskel et al., 2016; Mathias and Trugman, 2022). Thus, stronger regulation of canopy temperatures via evaporative cooling under hot, wet conditions is essential for sustaining physiological function. If plant-available moisture declines, dryland trees like those in the Kuiseb could become more vulnerable to thermal stress and its consequences.

The conceptual framework presented in Fig. 1 and explored in this study sheds light on a number of plant physiological responses to water and temperature stress that are missing in current model formulations of plant hydraulic behavior. Most process-based vegetation models used within Earth System Models rely on stomatal optimization theory, wherein plants regulate stomata to maximize carbon gain relative to a penalty for stomatal opening (Wang et al., 2020), to determine ecosystem-scale "stomatal" conductance. In these approaches, stomatal conductance is formulated as a function of a set of environmental variables—usually including VPD and CO₂. The penalty function ranges from functions focused on the cost of losing water to the cost of vascular damage, depending on the model. Models also include empirically derived parameters, such as m in Eq. (2) (Ball et al., 1987; Medlyn et al., 2011). These parameters are typically prescribed by plant functional type and play a key role in determining modeled ecosystem water and carbon fluxes (Zarakas et al., 2024; Fischer et al., 2011). However, our results indicate that parameters like m itself may be environmentally dependent. Moreover, the decoupling of water and

temperature regulation under hot, wet conditions suggests that plants in extreme environments may use water for purposes other than carbon assimilation, such as avoiding thermal stress. This result is consistent with observations of decoupling between transpiration and carbon uptake in other dryland species under high temperatures (Aparecido et al., 2020; Marchin et al., 2023). In light of forecasted increases in the prevalence of extreme environmental conditions across the globe, these findings highlight the need for comparing frameworks that account for plant responses to water and temperature stress within existing Earth System Model formulations.

5. Conclusion

Here, we introduced a co-regulation framework for evaluating the linkages between plant water and temperature regulation and showed that desert tree species have different responses to supply- and demand-driven water stress, but similar responses to thermal stress. By using fine-scale remote sensing retrievals of canopy temperature, conductance, and transpiration, we were able to resolve relationships between individual plant behaviors as well as community-scale patterns. Our findings indicate that plants must make tradeoffs between hydraulic function and avoiding thermal stress under most conditions. Thus, our framework holistically enables diagnoses of plant stress, accounting for responses to water supply and demand, as well as thermal stress.

Our findings highlight the importance of capturing plant responses to the full factorial of water and temperature stress, particularly given the future impacts of climate change. Unexpected plant behaviors emerge under isolated stresses (hot, wet and cool, dry conditions) that provide insight into the plasticity of water-use strategies. We showed that the more conservative *F. albida* trees exhibit plasticity in their response to dry conditions depending on atmospheric temperature and dryness, highlighting the importance of supply- and demand-side controls on hydraulic regulation. In addition, decoupling between regulation of water-use and temperature occurred when both supply and demand were high, indicating that evaporative cooling is an important mechanism for avoiding thermal stress in desert species, so long as water availability is sufficiently high. Thus, integrating the full range of supply- and demand-driven stresses is essential for understanding and accurately predicting plant and ecosystem responses to climate change, particularly given that both of these observed behaviors – an increase in conductance in water-sensitive species under cool, dry conditions and co-regulation of water and temperature under hot, wet conditions – are vulnerable to elevated atmospheric temperature and moisture demand and declining plant-available moisture. Finally, given predicted increases in hydrologic variability, VPD, and air temperatures in Southern Africa (Almazroui et al., 2020; Abiodun et al., 2019) and worldwide (Held and Soden, 2006; Douville et al., 2022), the strategies plants use to withstand extreme water and temperature stress like that experienced by Namib species provide a window into ecosystem function across the globe in a warmer, drier future.

CRediT authorship contribution statement

Bryn E. Morgan: Writing – review & editing, Writing – original draft, Visualization, Software, Methodology, Investigation, Funding acquisition, Formal analysis, Data curation, Conceptualization. **Anna T. Trugman:** Writing – review & editing, Writing – original draft, Methodology. **Kelly K. Taylor:** Writing – review & editing, Resources, Methodology, Investigation, Conceptualization.

Declaration of competing interest

The authors declare that they have no known competing financial interests or personal relationships that could have appeared to influence the work reported in this paper.

Acknowledgments

This work was funded by a Fulbright U.S. Student Grant awarded to B.E.M. and conducted in affiliation with Gobabeb Namib Research Institute in Namibia. The Fulbright Program is sponsored by the U.S. Department of State. This work is solely the responsibility of the authors and does not necessarily represent the official view of the Fulbright Program or the Government of the United States. B.E.M. also acknowledges funding support from the American Philosophical Society Lewis and Clark Fund for Exploration and Field Research and the University of California, Santa Barbara Department of Geography Leal Anne Kerry Mertes Award. B.E.M. and K.K.C. acknowledge funding from the Zegar Family Foundation (Grant No. SB200109). A.T.T. acknowledges funding from the National Science Foundation (Grant No. 2003205), the Gordon and Betty Moore Foundation (Grant No. GBMF11974), the USDI National Park Service (Award Nos. P24AC00910 and P24AC01425) and the CALFIRE Forest Health Research Program (Grant No. 60164685). We thank the scientists, staff, and support team at Gobabeb for facilitating this research. In particular, we acknowledge Ulrich Bezuidenhout for assistance with fieldwork and Gillian Maggs-Kölling and Eugène Marais for making this work possible. We thank Doug Bolger and Saima Shikesho (Dartmouth College) for their help in the field and Michael Singer (Cardiff University; University of California, Santa Barbara) and Dar Roberts (University of California, Santa Barbara) for their advice on the research design.

Appendix A. Supplementary data

Supplementary material related to this article can be found online at <https://doi.org/10.1016/j.agrformet.2025.110929>.

Data availability

Canopy temperature, conductance, and transpiration data are available at <https://doi.org/10.5281/zenodo.17563443>.

References

- Abiodun, B.J., Makhanya, N., Petja, B., Abatan, A.A., Oguntunde, P.G., 2019. Future projection of droughts over major river basins in southern Africa at specific global warming levels. *Theor. Appl. Climatol.* 137 (3–4), 1785–1799. <http://dx.doi.org/10.1007/s00704-018-2693-0>.
- Allen, C.D., Breshears, D.D., McDowell, N.G., 2015. On underestimation of global vulnerability to tree mortality and forest die-off from hotter drought in the anthropocene. *Ecosphere* 6 (8), art129. <http://dx.doi.org/10.1890/ES15-00203.1>.
- Almazroui, M., Saeed, F., Saeed, S., Nazrul Islam, M., Ismail, M., Klutse, N.A.B., Siddiqui, M.H., 2020. Projected change in temperature and precipitation over Africa from CMIP6. *Earth Syst. Environ.* 4 (3), 455–475. <http://dx.doi.org/10.1007/s41748-020-00161-x>.
- Anderegg, W.R.L., 2015. Spatial and temporal variation in plant hydraulic traits and their relevance for climate change impacts on vegetation. *New Phytol.* 205 (3), 1008–1014. <http://dx.doi.org/10.1111/nph.12907>.
- Anderegg, W.R.L., Kane, J.M., Anderegg, L.D.L., 2013. Consequences of widespread tree mortality triggered by drought and temperature stress. *Nat. Clim. Chang.* 3 (1), 30–36. <http://dx.doi.org/10.1038/nclimate1635>.
- Anderegg, W.R.L., Klein, T., Bartlett, M., Sack, L., Pellegrini, A.F., Choat, B., Jansen, S., 2016. Meta-analysis reveals that hydraulic traits explain cross-species patterns of drought-induced tree mortality across the globe. *Proc. Natl. Acad. Sci. USA* 113 (18), 5024–5029. <http://dx.doi.org/10.1073/pnas.1525678113>.
- Anderegg, W.R.L., Konings, A.G., Trugman, A.T., Yu, K., Bowling, D.R., Gabbitas, R., Karp, D.S., Pacala, S., Sperry, J.S., Sulman, B.N., Zenes, N., 2018. Hydraulic diversity of forests regulates ecosystem resilience during drought. *Nature* 561 (7724), 538–541. <http://dx.doi.org/10.1038/s41586-018-0539-7>.
- Anderegg, W.R.L., Meinzer, F.C., 2015. Wood anatomy and plant hydraulics in a changing climate. In: Hacke, U. (Ed.), *Functional and Ecological Xylem Anatomy*. Springer International Publishing, Cham, pp. 235–253. http://dx.doi.org/10.1007/978-3-319-15783-2_9.
- Anderegg, W.R.L., Venturas, M.D., 2020. Plant hydraulics play a critical role in Earth system fluxes. *New Phytol.* 226 (6), 1535–1538. <http://dx.doi.org/10.1111/nph.16548>.
- Aparecido, L.M.T., Woo, S., Suazo, C., Hultine, K.R., Blonder, B., 2020. High water use in desert plants exposed to extreme heat. *Ecol. Lett.* 23 (8), 1189–1200. <http://dx.doi.org/10.1111/ele.13516>.
- Arnold, S., Attinger, S., Frank, K., Baxter, P., Possingham, H., Hildebrandt, A., 2016. Ecosystem management along ephemeral rivers: Trading off socio-economic water supply and vegetation conservation under flood regime uncertainty. *River Res. Appl.* 32, 216–233. <http://dx.doi.org/10.1002/rra.2853>.
- Arnold, S., Attinger, S., Frank, K., Hildebrandt, A., 2009. Uncertainty in parameterisation and model structure affect simulation results in coupled ecohydrological models. *Hydrol. Earth Syst. Sci.* 13 (10), 1789–1807. <http://dx.doi.org/10.5194/hess-13-1789-2009>.
- Ball, J.T., Woodrow, I.E., Berry, J.A., 1987. A model predicting stomatal conductance and its contribution to the control of photosynthesis under different environmental conditions. In: Biggins, J. (Ed.), *Progress in Photosynthesis Research*. In: *Proceedings of the VIIth International Congress on Photosynthesis*, vol. 4, Springer, Dordrecht, pp. 221–224. http://dx.doi.org/10.1007/978-94-017-0519-6_48.
- Barnes, R., Fagg, C., Milton, S., 1997. *Acacia Erioloba: Monograph and Annotated Bibliography*. Oxford Forestry Institute, University of Oxford.
- Bate, G., Walker, B., 1993. *Water relations of the vegetation along the Kuiseb River, Namibia*. Madoqua 18 (2), 85–91.
- Berg, A., Findell, K., Lintner, B., Giannini, A., Seneviratne, S.I., van den Hurk, B., Lorenz, R., Pitman, A., Hagemann, S., Meier, A., Cheruy, F., Ducharme, A., Malyshev, S., Milly, P.C.D., 2016. Land-atmosphere feedbacks amplify aridity increase over land under global warming. *Nat. Clim. Chang.* 6 (9), 869–874. <http://dx.doi.org/10.1038/nclimate3029>.
- Berger-Landefeldt, U., 1936. *Der wasserhaushalt der alpenpflanzen (the water budget of alpine plants)*. In: *Bibliotheca Botanica. Schweizerbart Science Publishers*.
- Berni, J.A., Zarco-Tejada, P.J., Suárez, L., Fereres, E., 2009. Thermal and narrowband multispectral remote sensing for vegetation monitoring from an unmanned aerial vehicle. *IEEE Trans. Geosci. Remote Sens.* 47 (3), 722–738. <http://dx.doi.org/10.1109/TGRS.2008.2010457>.
- Berry, J., Bjorkman, O., 1980. Photosynthetic response and adaptation to temperature in higher plants. *Annu. Rev. Plant Physiol.* 31 (1), 491–543. <http://dx.doi.org/10.1146/annurev.pp.31.060180.002423>.
- Blonder, B.W., Michaletz, S.T., 2018. A model for leaf temperature decoupling from air temperature. *Agricultur. Forest. Meterol.* 262, 354–360. <http://dx.doi.org/10.1016/j.agrformet.2018.07.012>.
- Bonan, G.B., 2008. Forests and climate change: Forcings, feedbacks, and the climate benefits of forests. *Science* 320 (5882), 1444–1449. <http://dx.doi.org/10.1126/science.1155121>.
- Canadell, J., Jackson, R.B., Ehleringer, J.R., Mooney, H.A., Sala, O.E., Schulze, E.-D., 1996. Maximum rooting depth of vegetation types at the global scale. *Oecologia* 108 (4), 583–595. <http://dx.doi.org/10.1007/BF00329030>.
- Choat, B., Jansen, S., Brodrribb, T.J., Cochard, H., Delzon, S., Bhaskar, R., Bucci, S.J., Feild, T.S., Gleason, S.M., Hacke, U.G., Jacobsen, A.L., Lens, F., Maherli, H., Martínez-Vilalta, J., Mayr, S., Mencuccini, M., Mitchell, P.J., Nardini, A., Pittermann, J., Pratt, R.B., Sperry, J.S., Westoby, M., Wright, I.J., Zanne, A.E., 2012. Global convergence in the vulnerability of forests to drought. *Nature* 491 (7426), 752–755. <http://dx.doi.org/10.1038/nature11688>.
- Coates Palgrave, K., 2002. *Trees of Southern Africa*. Struik, Cape Town.
- Cochard, H., 2021. A new mechanism for tree mortality due to drought and heatwaves. *Peer Community J. 1*, <http://dx.doi.org/10.24072/pcjournal.45>.
- Cook, A.M., Berry, N., Milner, K.V., Leigh, A., 2021. Water availability influences thermal safety margins for leaves. *Funct. Ecol.* 35 (10), 2179–2189. <http://dx.doi.org/10.1111/1365-2435.13868>.
- Cunningham, S.C., 2004. Stomatal sensitivity to vapour pressure deficit of temperate and tropical evergreen rainforest trees of Australia. *Trees* 18 (4), 399–407. <http://dx.doi.org/10.1007/s00468-004-0318-y>.
- Dahan, O., Tatarsky, B., Enzel, Y., Kulls, C., Seely, M., Benito, G., 2008. Dynamics of flood water infiltration and ground water recharge in hyperarid desert. *Ground Water* 46 (3), 450–461. <http://dx.doi.org/10.1111/j.1745-6584.2007.00414.x>.
- Dai, A., 2006. Recent climatology, variability, and trends in global surface humidity. *J. Clim.* 19 (15), 3589–3606. <http://dx.doi.org/10.1175/JCLI3816.1>.
- Dai, A., 2013. Increasing drought under global warming in observations and models. *Nat. Clim. Chang.* 3 (1), 52–58. <http://dx.doi.org/10.1038/nclimate1633>.
- Doughty, C.E., Goulden, M.L., 2008. Are tropical forests near a high temperature threshold? *J. Geophys. Res.: Biogeosciences* 113 (G1), <http://dx.doi.org/10.1029/2007JG000632>.
- Doughty, C.E., Keany, J.M., Wiebe, B.C., Rey-Sánchez, C., Carter, K.R., Middleby, K.B., Cheeseman, A.W., Goulden, M.L., da Rocha, H.R., Miller, S.D., Malhi, Y., Faust, S., Gloor, E., Slot, M., Oliveras Menor, I., Crous, K.Y., Goldsmith, G.R., Fisher, J.B., 2023. Tropical forests are approaching critical temperature thresholds. *Nature* 1–7. <http://dx.doi.org/10.1038/s41586-023-06391-z>.
- Douville, H., Qasmi, S., Ribes, A., Bock, O., 2022. Global warming at near-constant tropospheric relative humidity is supported by observations. *Commun. Earth & Environ.* 3 (1), 1–7. <http://dx.doi.org/10.1038/s43247-022-00561-z>.
- Drake, J.E., Harwood, R., Värvhammar, A., Barbour, M.M., Reich, P.B., Barton, C.V.M., Tjoelker, M.G., 2020. No evidence of homeostatic regulation of leaf temperature in eucalyptus *parra-mattensis* trees: Integration of CO₂ flux and oxygen isotope methodologies. *New Phytol.* 228 (5), 1511–1523. <http://dx.doi.org/10.1111/nph.16733>.

- Dupuy, N.C., Dreyfus, B.L., 1992. Bradyrhizobium populations occur in deep soil under the leguminous tree *acacia albida*. *Applied and Environmental Microbiology* 58 (8), 2415–2419. <http://dx.doi.org/10.1128/aem.58.8.2415-2419.1992>.
- Eamus, D., Boulain, N., Cleverly, J., Breshears, D.D., 2013. Global change-type drought-induced tree mortality: Vapor pressure deficit is more important than temperature per se in causing decline in tree health. *Ecol. Evol.* 3 (8), 2711–2729. <http://dx.doi.org/10.1002/ece3.664>.
- Feng, X., Ackerly, D.D., Dawson, T.E., Manzoni, S., McLaughlin, B., Skelton, R.P., Vico, G., Weitz, A.P., Thompson, S.E., 2019. Beyond isohydricity: The role of environmental variability in determining plant drought responses. *Plant, Cell & Environ.* 42 (4), 1104–1111. <http://dx.doi.org/10.1111/pce.13486>.
- Field, C.B., Barros, V., Stocker, T.F., Dahe, Q., 2012. Managing the Risks of Extreme Events and Disasters to Advance Climate Change Adaptation: Special Report of the Intergovernmental Panel on Climate Change. Cambridge University Press, Cambridge, <http://dx.doi.org/10.1017/CBO9781139177245>.
- Fischer, E.M., Lawrence, D.M., Sanderson, B.M., 2011. Quantifying uncertainties in projections of extremes—a perturbed land surface parameter experiment. *Clim. Dyn.* 37 (7), 1381–1398. <http://dx.doi.org/10.1007/s00382-010-0915-y>.
- Fontes, C.G., Dawson, T.E., Jardine, K., McDowell, N., Gimenez, B.O., Anderegg, L., Negrón-Juárez, R., Higuchi, N., Fine, P.V.A., Aratijo, A.C., Chambers, J.Q., 2018. Dry and hot: The hydraulic consequences of a climate change-type drought for amazonian trees. *Phil. Trans. R. Soc. B* 373 (1760), 20180209. <http://dx.doi.org/10.1098/rstb.2018.0209>.
- Gates, D.M., 1968. Transpiration and leaf temperature. *Annu. Rev. Plant Physiol.* 19 (1), 211–238. <http://dx.doi.org/10.1146/annurev.pp.19.060168.001235>.
- Gauthier, A., Kahmen, A., Limousin, J.-M., Vilagrosa, A., Didion-Gency, M., Mas, E., Milano, A., Tunas, A., Grossiord, C., 2024. High heat tolerance, evaporative cooling, and stomatal decoupling regulate canopy temperature and their safety margins in three European oak species. *Global Change Biol.* 30 (8), e17439. <http://dx.doi.org/10.1111/gcb.17439>.
- Grödek, T., Morin, E., Helman, D., Lensky, I., Dahan, O., Seely, M., Benito, G., Enzel, Y., 2020. Eco-hydrology and geomorphology of the largest floods along the hyperarid kuseb river, namibia. *J. Hydrol.* 582 (July 2019), 124450. <http://dx.doi.org/10.1016/j.jhydrol.2019.124450>.
- Grossiord, C., Buckley, T.N., Cernusak, L.A., Novick, K.A., Poulter, B., Siegwolf, R.T., Sperry, J.S., McDowell, N.G., 2020. Plant responses to rising vapor pressure deficit. *New Phytol.* 226 (6), 1550–1566. <http://dx.doi.org/10.1111/nph.16485>.
- Grossiord, C., Gessler, A., Reed, S.C., Borrego, I., Collins, A.D., Dickman, L.T., Ryan, M., Schönbeck, L., Sevanto, S., Vilagrosa, A., McDowell, N.G., 2018. Reductions in tree performance during hotter droughts are mitigated by shifts in nitrogen cycling. *Plant, Cell & Environ.* 41 (11), 2627–2637. <http://dx.doi.org/10.1111/pce.13389>.
- Grossiord, C., Sevanto, S., Borrego, I., Chan, A.M., Collins, A.D., Dickman, L.T., Hudson, P.J., McBranch, N., Michaletz, S.T., Pockman, W.T., Ryan, M., Vilagrosa, A., McDowell, N.G., 2017. Tree water dynamics in a drying and warming world. *Plant, Cell & Environ.* 40 (9), 1861–1873. <http://dx.doi.org/10.1111/pce.12991>.
- Guo, Z., Still, C.J., Lee, C.K.F., Ryu, Y., Blonder, B., Wang, J., Bonebrake, T.C., Hughes, A., Li, Y., Yeung, H.C.H., Zhang, K., Law, Y.K., Lin, Z., Wu, J., 2023. Does plant ecosystem thermoregulation occur? an extratropical assessment at different spatial and temporal scales. *New Phytol.* 238 (3), 1004–1018. <http://dx.doi.org/10.1111/nph.18632>.
- Hacke, U.G., Sperry, J.S., Pockman, W.T., Davis, S.D., McCulloch, K.A., 2001. Trends in wood density and structure are linked to prevention of xylem implosion by negative pressure. *Oecologia* 126 (4), 457–461. <http://dx.doi.org/10.1007/s004420100628>.
- Held, I.M., Soden, B.J., 2006. Robust responses of the hydrological cycle to global warming. *J. Clim.* 19 (21), 5686–5699. <http://dx.doi.org/10.1175/JCLI3990.1>.
- Heskell, M.A., O'Sullivan, O.S., Reich, P.B., Tjoelker, M.G., Weerasinghe, L.K., Penillard, A., Egerton, J.J.G., Creek, D., Bloomfield, K.J., Xiang, J., Sinca, F., Stangl, Z.R., Martinez-de la Torre, A., Griffin, K.L., Huntingford, C., Hurry, V., Meir, P., Turnbull, M.H., Atkin, O.K., 2016. Convergence in the temperature response of leaf respiration across biomes and plant functional types. *Proc. Natl. Acad. Sci.* 113 (14), 3832–3837. <http://dx.doi.org/10.1073/pnas.1520282113>.
- Huntley, B.J., 1985. The kuseb environment: The development of a monitoring baseline.. 106, (Committee for Terrestrial Ecosystems), National Scientific Programmes Unit: CSIR, pp. 1–138.
- IPCC, 2023. Climate Change 2021 – The Physical Science Basis: Working Group I Contribution to the Sixth Assessment Report of the Intergovernmental Panel on Climate Change, first ed. Cambridge University Press, <http://dx.doi.org/10.1017/9781009157896>.
- Jacobsen, A.L., Agenbag, L., Esler, K.J., Pratt, R.B., Ewers, F.W., Davis, S.D., 2007. Xylem density, biomechanics and anatomical traits correlate with water stress in 17 evergreen shrub species of the mediterranean-type climate region of South Africa. *J. Ecol.* 95 (1), 171–183. <http://dx.doi.org/10.1111/j.1365-2745.2006.01186.x>.
- Jacobson, P.J., Jacobson, K.M., Angermeier, P.L., Cherry, D.S., 2000. Hydrologic influences on soil properties along ephemeral rivers in the namib desert. *J. Arid. Environ.* 45 (1), 21–34. <http://dx.doi.org/10.1006/jare.1999.0619>.
- Jones, H., 1980. Interaction and integration of adaptive responses to water stress: the implications of an unpredictable environment. In: Turner, N., Kramer, P. (Eds.), *Adaptation of Plants To Water and High Temperature Stress*. Wiley, pp. 353–365.
- Jung, M., Reichstein, M., Ciais, P., Seneviratne, S.I., Sheffield, J., Goulden, M.L., Bonan, G., Cescatti, A., Chen, J., De Jeu, R., Dolman, A.J., Eugster, W., Gerten, D., Gianelle, D., Gobron, N., Heinke, J., Kimball, J., Law, B.E., Montagnani, L., Mu, Q., Mueller, B., Oleson, K., Papale, D., Richardson, A.D., Roupsard, O., Running, S., Tomelleri, E., Viovy, N., Weber, U., Williams, C., Wood, E., Zaehle, S., Zhang, K., 2010. Recent decline in the global land evapotranspiration trend due to limited moisture supply. *Nature* 467 (7318), 951–954. <http://dx.doi.org/10.1038/nature09396>.
- Kibler, C.L., Trugman, A.T., Roberts, D.A., Still, C.J., Scott, R.L., Caylor, K.K., Stella, J.C., Singer, M.B., 2023. Evapotranspiration regulates leaf temperature and respiration in dryland vegetation. *Agricul. Forest. Meterol.* 339, 109560. <http://dx.doi.org/10.1016/j.agrformet.2023.109560>.
- Kitudom, N., Fauset, S., Zhou, Y., Fan, Z., Li, M., He, M., Zhang, S., Xu, K., Lin, H., 2022. Thermal safety margins of plant leaves across biomes under a heatwave. *Sci. Total Environ.* 806, 150416. <http://dx.doi.org/10.1016/j.scitotenv.2021.150416>.
- Krause, G.H., Winter, K., Krause, B., Jahns, P., García, M., Aranda, J., Virgo, A., 2010. High-temperature tolerance of a tropical tree, *ficus insipida*: Methodological reassessment and climate change considerations. *Funct. Plant Biology* 37 (9), 890–900. <http://dx.doi.org/10.1071/FP10034>.
- Kustas, W., Anderson, M., 2009. Advances in thermal infrared remote sensing for land surface modeling. *Agricul. Forest. Meterol.* 149 (12), 2071–2081. <http://dx.doi.org/10.1016/j.agrformet.2009.05.016>.
- Lange, J., 2005. Dynamics of transmission losses in a large arid stream channel. *J. Hydrol.* 306 (1–4), 112–126. <http://dx.doi.org/10.1016/j.jhydrol.2004.09.016>.
- Lin, H., Chen, Y., Zhang, H., Fu, P., Fan, Z., 2017. Stronger cooling effects of transpiration and leaf physical traits of plants from a hot dry habitat than from a hot wet habitat. *Funct. Ecol.* 31 (12), 2202–2211. <http://dx.doi.org/10.1111/1365-2435.12923>.
- Linacre, E.T., 1964. A note on a feature of leaf and air temperatures. *Agric. Meteorol.* 1 (1), 66–72. [http://dx.doi.org/10.1016/0002-1571\(64\)90009-3](http://dx.doi.org/10.1016/0002-1571(64)90009-3).
- Liu, L., Gudmundsson, L., Hauser, M., Qin, D., Li, S., Seneviratne, S.I., 2020a. Soil moisture dominates dryness stress on ecosystem production globally. *Nat. Commun.* 11 (1), 4892. <http://dx.doi.org/10.1038/s41467-020-18631-1>.
- Liu, Y., Kumar, M., Katul, G.G., Feng, X., Konings, A.G., 2020b. Plant hydraulics accentuates the effect of atmospheric moisture stress on transpiration. *Nat. Clim. Chang.* 10 (7), 691–695. <http://dx.doi.org/10.1038/s41558-020-0781-5>.
- Ludlow, M., 1989. Strategies of response to water stress. In: Kreeb, K., Richter, H., Hinckley, T. (Eds.), *Structural and Functional Responses To Environmental Stresses*. Academic Publishers, pp. 27–52.
- Mahan, J.R., Upchurch, D.R., 1988. Maintenance of constant leaf temperature by plants—I. hypothesis-limited homeothermy. *Environ. Exp. Bot.* 28 (4), 351–357. [http://dx.doi.org/10.1016/0098-8472\(88\)90059-7](http://dx.doi.org/10.1016/0098-8472(88)90059-7).
- Maherali, H., Delucia, E.H., 2001. Influence of climate-driven shifts in biomass allocation on water transport and storage in ponderosa pine. *Oecologia* 129 (4), 481–491. <http://dx.doi.org/10.1007/s004420100758>.
- Marchin, R.M., Medlyn, B.E., Tjoelker, M.G., Ellsworth, D.S., 2023. Decoupling between stomatal conductance and photosynthesis occurs under extreme heat in broadleaf tree species regardless of water access. *Global Change Biol.* n/a (n/a), <http://dx.doi.org/10.1111/gcb.16929>.
- Martínez-Vilalta, J., Cochard, H., Mencuccini, M., Sterck, F., Herrero, A., Korhonen, J.F.J., Llorens, P., Nikinmaa, E., Nolé, A., Poyatos, R., Ripullone, F., Sassi-Klaassen, U., Zweifel, R., 2009. Hydraulic adjustment of scots pine across Europe. *New Phytol.* 184 (2), 353–364. <http://dx.doi.org/10.1111/j.1469-8137.2009.02954.x>.
- Mathias, J.M., Trugman, A.T., 2022. Climate change impacts plant carbon balance, increasing mean future carbon use efficiency but decreasing total forest extent at dry range edges. *Ecol. Lett.* 25 (2), 498–508. <http://dx.doi.org/10.1111/ele.13945>.
- Mau, A.C., Reed, S.C., Wood, T.E., Cavalieri, M.A., 2018. Temperate and tropical forest canopies are already functioning beyond their thermal thresholds for photosynthesis. *Forests* 9 (1), 47. <http://dx.doi.org/10.3390/f9010047>.
- McCabe, M.F., Rodell, M., Alsdorf, D.E., Miralles, D.G., Uijlenhoet, R., Wagner, W., Lucieer, A., Houborg, R., Verhoest, N.E., Franz, T.E., Shi, J., Gao, H., Wood, E.F., 2017. The future of earth observation in hydrology. *Hydrol. Earth Syst. Sci.* 21 (7), 3879–3914. <http://dx.doi.org/10.5194/hess-21-3879-2017>.
- McDowell, N., Pockman, W.T., Allen, C.D., Breshears, D.D., Cobb, N., Kolb, T., Plaut, J., Sperry, J., West, A., Williams, D.G., Yepez, E.A., 2008. Mechanisms of plant survival and mortality during drought: Why do some plants survive while others succumb to drought? *New Phytol.* 178 (4), 719–739. <http://dx.doi.org/10.1111/j.1469-8137.2008.02436.x>.
- Medlyn, B.E., Dreyer, E., Ellsworth, D., Forstreuter, M., Harley, P.C., Kirschbaum, M.U.F., Le Roux, X., Mont pied, P., Strassmeyer, J., Walcroft, A., Wang, K., Loustau, D., 2002. Temperature response of parameters of a biochemically based model of photosynthesis. II. a review of experimental data. *Plant, Cell & Environ.* 25 (9), 1167–1179. <http://dx.doi.org/10.1046/j.1365-3040.2002.00891.x>.
- Medlyn, B.E., Duursma, R.A., Eamus, D., Ellsworth, D.S., Prentice, I.C., Barton, C.V.M., Crous, K.Y., De Angelis, P., Freeman, M., Wingate, L., 2011. Reconciling the optimal and empirical approaches to modelling stomatal conductance. *Global Change Biol.* 17 (6), 2134–2144. <http://dx.doi.org/10.1111/j.1365-2486.2010.02375.x>.

- Meinzer, F.C., Woodruff, D.R., Marias, D.E., Smith, D.D., McCulloh, K.A., Howard, A.R., Magedman, A.L., 2016. Mapping 'hydroscapes' along the iso- to anisohydric continuum of stomatal regulation of plant water status. *Ecol. Lett.* 19 (11), 1343–1352. <http://dx.doi.org/10.1111/ele.12670>.
- Mencuccini, M., Manzoni, S., Christoffersen, B., 2019. Modelling water fluxes in plants: From tissues to biosphere. *New Phytol.* 222 (3), 1207–1222. <http://dx.doi.org/10.1111/nph.15681>.
- Michaletz, S.T., Weiser, M.D., McDowell, N.G., Zhou, J., Kaspari, M., Helliiker, B.R., Enquist, B.J., 2016. The energetic and carbon economic origins of leaf thermoregulation. *Nat. Plants* 2 (9), 1–9. <http://dx.doi.org/10.1038/nplants.2016.129>.
- Monteith, J.L., 1965. Evaporation and environment. In: *Symposia of the Society for Experimental Biology*. (19), Cambridge University Press, Cambridge, pp. 205–234.
- Monteith, J.L., 1995. A reinterpretation of stomatal responses to humidity. *Plant, Cell & Environ.* 18 (4), 357–364. <http://dx.doi.org/10.1111/j.1365-3040.1995.tb00371.x>.
- Morgan, B.E., 2023. Aeroet.
- Morgan, B.E., Bolger, D.T., Chipman, J.W., Dietrich, J.T., 2020. Lateral and longitudinal distribution of riparian vegetation along an ephemeral river in Namibia using remote sensing techniques. *J. Arid. Environ.* 181 (September 2020), 104220. <http://dx.doi.org/10.1016/j.jaridenv.2020.104220>.
- Morgan, B.E., Caylor, K.K., 2023. Estimating fine-scale transpiration from UAV-derived thermal imagery and atmospheric profiles. *Water Resour. Res.* 59 (11), <http://dx.doi.org/10.1029/2023WR035251>.
- Morgan, B.E., Chipman, J.W., Bolger, D.T., Dietrich, J.T., 2021. Spatiotemporal analysis of vegetation cover change in a large ephemeral river: Multi-sensor fusion of unmanned aerial vehicle (UAV) and landsat imagery. *Remote. Sens.* 13 (1), 1–24. <http://dx.doi.org/10.3390/rs13010051>.
- Morin, E., Grodek, T., Dahan, O., Benito, G., Kulls, C., Jacoby, Y., Langenhove, G.V., Seely, M., Enzel, Y., 2009. Flood routing and alluvial aquifer recharge along the ephemeral arid kuseb river, namibia. *J. Hydrol.* 368 (1–4), 262–275. <http://dx.doi.org/10.1016/j.jhydrol.2009.02.015>.
- Mrad, A., Sevanto, S., Domec, J.-C., Liu, Y., Nakad, M., Katul, G., 2019. A dynamic optimality principle for water use strategies explains isohydric to anisohydric plant responses to drought. *Front. For. Glob. Chang.* 2.
- Natural Resources Canada Canadian Geodetic Survey, 2022. Candadian spatial reference system precise point positioning.
- Novick, K.A., Ficklin, D.L., Stoy, P.C., Williams, C.A., Bohrer, G., Oishi, A.C., Papuga, S.A., Blanken, P.D., Noormets, A., Sulman, B.N., Scott, R.L., Wang, L., Phillips, R.P., 2016. The increasing importance of atmospheric demand for ecosystem water and carbon fluxes. *Nat. Clim. Chang.* 6 (11), 1023–1027. <http://dx.doi.org/10.1038/nclimate3114>.
- Oren, R., Sperry, J.S., Katul, G.G., Pataki, D.E., Ewers, B.E., Phillips, N., Schäfer, K.V.R., 1999. Survey and synthesis of intra- and interspecific variation in stomatal sensitivity to vapour pressure deficit. *Plant, Cell & Environ.* 22 (12), 1515–1526. <http://dx.doi.org/10.1046/j.1365-3040.1999.00513.x>.
- O'Sullivan, O.S., Heskell, M.A., Reich, P.B., Tjoelker, M.G., Weerasinghe, L.K., Penillard, A., Zhu, L., Egerton, J.J.G., Bloomfield, K.J., Creek, D., Bahar, N.H.A., Griffin, K.L., Hurry, V., Meir, P., Turnbull, M.H., Atkin, O.K., 2017. Thermal limits of leaf metabolism across biomes. *Global Change Biol.* 23 (1), 209–223. <http://dx.doi.org/10.1111/gcb.13477>.
- Pau, S., Dettò, M., Kim, Y., Still, C.J., 2018. Tropical forest temperature thresholds for gross primary productivity. *Ecosphere* 9 (7), e02311. <http://dx.doi.org/10.1002/ecs2.2311>.
- Peng, C., Zeng, J., Chen, K.-S., Li, Z., Ma, H., Zhang, X., Shi, P., Wang, T., Yi, L., Bi, H., 2023. Global spatiotemporal trend of satellite-based soil moisture and its influencing factors in the early 21st century. *Remote Sens. Environ.* 291, 113569. <http://dx.doi.org/10.1016/j.rse.2023.113569>.
- Penman, H.L., 1948. Natural evaporation from open water, bare soil and grass. *Proc. R. Soc. Lond. Ser. A. Math. Phys. Sci.* 193 (1032), 120–145.
- Poyatos, R., Martínez-Vilalta, J., Čermák, J., Ceulemans, R., Granier, A., Irvine, J., Köstner, B., Lagergren, F., Meiresonne, L., Nadezhdin, N., Zimmermann, R., Llorens, P., Mencuccini, M., 2007. Plasticity in hydraulic architecture of Scots pine across eurasia. *Oecologia* 153 (2), 245–259. <http://dx.doi.org/10.1007/s00442-007-0740-0>.
- Pritzkow, C., Williamson, V., Szota, C., Trouvé, R., Arndt, S.K., 2020. Phenotypic plasticity and genetic adaptation of functional traits influences intra-specific variation in hydraulic efficiency and safety. *Tree Physiol.* 40 (2), 215–229. <http://dx.doi.org/10.1093/treephys/tpz121>.
- Roman, D.T., Novick, K.A., Brzostek, E.R., Dragoni, D., Rahman, F., Phillips, R.P., 2015. The role of isohydric and anisohydric species in determining ecosystem-scale response to severe drought. *Oecologia* 179 (3), 641–654. <http://dx.doi.org/10.1007/s00442-015-3380-9>.
- Roupsard, O., Ferhi, A., Granier, A., Pallo, F., Depommier, D., Mallet, B., Joly, H.I., Dreyer, E., 1999. Reverse phenology and dry-season water uptake by faidherbia albida (del.) a. chev. in an agroforestry parkland of sudanese west africa. *Funct. Ecol.* 13 (4), 460–472. <http://dx.doi.org/10.1046/j.1365-2435.1999.00345.x>.
- Running, S.W., 1976. Environmental control of leaf water conductance in conifers. *Can. J. Forest Res.* 6 (1), 104–112. <http://dx.doi.org/10.1139/x76-013>.
- Schachtschneider, K., 2010. Water Sourcing by Riparian Trees along Ephemeral Riverbeds (Ph.D. thesis). University of Cape Town.
- Schachtschneider, K., February, E.C., 2010. The relationship between fog, floods, groundwater and tree growth along the lower kuseb river in the hyperarid namib. *J. Arid. Environ.* 74 (12), 1632–1637. <http://dx.doi.org/10.1016/j.jaridenv.2010.05.027>.
- Schönbeck, L.C., Schuler, P., Lehmann, M.M., Mas, E., Mekarni, L., Pivovaroff, A.L., Turberg, P., Grossjord, C., 2022. Increasing temperature and vapour pressure deficit lead to hydraulic damages in the absence of soil drought. *Plant, Cell & Environ.* 45 (11), 3275–3289. <http://dx.doi.org/10.1111/pce.14425>.
- Seely, M.K., Buskirk, W., Hamilton, W., Dixon, J., 1981. Lower kuseb river perennial vegetation survey. *J. The South Afr. Afr. Sci. Soc.* XXXIV/XXXV, 57–86.
- Seneviratne, S.I., Corti, T., Davin, E.L., Hirschi, M., Jaeger, E.B., Lehner, I., Orłowsky, B., Teuling, A.J., 2010. Investigating soil moisture-climate interactions in a changing climate: A review. *Earth-Sci. Rev.* 99 (3), 125–161. <http://dx.doi.org/10.1016/j.earscirev.2010.02.004>.
- Sherwood, S., Fu, Q., 2014. A drier future? *Science* 343 (6172), 737–739. <http://dx.doi.org/10.1126/science.1247620>.
- Simpson, I.R., McKinnon, K.A., Kennedy, D., Lawrence, D.M., Lehner, F., Seager, R., 2024. Observed humidity trends in dry regions contradict climate models. *Proc. Natl. Acad. Sci.* 121 (1), e2302480120. <http://dx.doi.org/10.1073/pnas.2302480120>.
- Slot, M., Cala, D., Aranda, J., Virgo, A., Michaletz, S.T., Winter, K., 2021. Leaf heat tolerance of 147 tropical forest species varies with elevation and leaf functional traits, but not with phylogeny. *Plant, Cell & Environ.* 44 (7), 2414–2427. <http://dx.doi.org/10.1111/pce.14060>.
- Slot, M., Winter, K., 2017. In situ temperature response of photosynthesis of 42 tree and liana species in the canopy of two panamanian lowland tropical forests with contrasting rainfall regimes. *New Phytol.* 214 (3), 1103–1117. <http://dx.doi.org/10.1111/nph.14469>.
- Southern African Science Service Centre for Climate Change and Adaptive Land Management WeatherNet, 2023. Gobabeb met daily values.
- Sperry, J.S., Hacke, U.G., Oren, R., Comstock, J.P., 2002. Water deficits and hydraulic limits to leaf water supply. *Plant, Cell & Environ.* 25 (2), 251–263. <http://dx.doi.org/10.1046/j.0016-8025.2001.00799.x>.
- Still, C.J., Page, G., Rastogi, B., Griffith, D.M., Aubrecht, D.M., Kim, Y., Burns, S.P., Hanson, C.V., Kwon, H., Hawkins, L., Meinzer, F.C., Sevanto, S., Roberts, D., Goulden, M., Pau, S., Dettò, M., Helliiker, B., Richardson, A.D., 2022. No evidence of canopy-scale leaf thermoregulation to cool leaves below air temperature across a range of forest ecosystems. *Proc. Natl. Acad. Sci.* 119 (38), e2205682119. <http://dx.doi.org/10.1073/pnas.2205682119>.
- Sulman, B.N., Roman, D.T., Yi, K., Wang, L., Phillips, R.P., Novick, K.A., 2016. High atmospheric demand for water can limit forest carbon uptake and transpiration as severely as dry soil. *Geophys. Res. Lett.* 43 (18), 9686–9695. <http://dx.doi.org/10.1002/2016GL069416>.
- Tardieu, F., Simonneau, T., 1998. Variability among species of stomatal control under fluctuating soil water status and evaporative demand: Modelling isohydric and anisohydric behaviours. *J. Exp. Bot.* 49 (Special Issue), 419–432. http://dx.doi.org/10.1093/jxb/49.Special_Issue.419.
- Theron, G.K., van Rooyen, N., van Rooyen, M.W., 1980. Vegetation of the lower kuseb river. *Madoqua* 11 (4), 327–345.
- Theron, G.K., van Rooyen, N., van Rooyen, M.W., Jankowitz, W.J., 1985. Vegetation structure and vitality in the lower kuseb. In: Huntley, B.J. (Ed.), *The Kuseb Environment: The Development Ofa Monitoring Baseline*. CSIR, National Scientific Programmes Unit, pp. 81–91.
- Timberlake, J., Fagg, C., Barnes, R., 1999. *Field Guide to the Acacias of Zimbabwe*. CBS Publishing, Harare, Zimbabwe.
- Trugman, A.T., Medvigy, D., Mankin, J.S., Anderegg, W.R.L., 2018. Soil moisture stress as a major driver of carbon cycle uncertainty. *Geophys. Res. Lett.* 45 (13), 6495–6503. <http://dx.doi.org/10.1029/2018GL078131>.
- Upchurch, D.R., Mahan, J.R., 1988. Maintenance of constant leaf temperature by plants—II: experimental observations in cotton. *Environ. Exp. Bot.* 28 (4), 359–366. [http://dx.doi.org/10.1016/0098-8472\(88\)90060-3](http://dx.doi.org/10.1016/0098-8472(88)90060-3).
- Urban, J., Ingwers, M.W., McGuire, M.A., Teskey, R.O., 2017. Increase in leaf temperature opens stomata and decouples net photosynthesis from stomatal conductance in pinus taeda and populus deltoides x nigra. *J. Exp. Bot.* 68 (7), 1757–1767. <http://dx.doi.org/10.1093/jxb/erx052>.
- Wang, Y., Sperry, J.S., Anderegg, W.R.L., Venturas, M.D., Trugman, A.T., 2020. A theoretical and empirical assessment of stomatal optimization modeling. *New Phytol.* 227 (2), 311–325. <http://dx.doi.org/10.1111/nph.16572>.
- Ward, J.D., Breen, C.M., 1983. Drought stress and the demise of acacia albida along the lower kuseb river, central namib desert: Preliminary findings. *South Afr. J. Sci.* 79 (11), 444–447.
- Way, D.A., Yamori, W., 2014. Thermal acclimation of photosynthesis: On the importance of adjusting our definitions and accounting for thermal acclimation of respiration. *Photosynth. Res.* 119 (1), 89–100. <http://dx.doi.org/10.1007/s11120-013-9873-7>.
- Williams, A.P., Allen, C.D., Macalady, A.K., Griffin, D., Woodhouse, C.A., Meko, D.M., Swetnam, T.W., Rauscher, S.A., Seager, R., Grissino-Mayer, H.D., Dean, J.S., Cook, E.R., Gangodagamage, C., Cai, M., McDowell, N.G., 2013. Temperature as a potent driver of regional forest drought stress and tree mortality. *Nat. Clim. Chang.* 3 (3), 292–297. <http://dx.doi.org/10.1038/nclimate1693>.

- Yamori, W., Hikosaka, K., Way, D.A., 2014. Temperature response of photosynthesis in C3, C4, and CAM plants: Temperature acclimation and temperature adaptation. *Photosynth. Res.* 119 (1), 101–117. <http://dx.doi.org/10.1007/s11120-013-9874-6>.
- Yi, K., Smith, J.W., Jablonski, A.D., Tatham, E.A., Scanlon, T.M., Lerdau, M.T., Novick, K.A., Yang, X., 2020. High heterogeneity in canopy temperature among co-occurring tree species in a temperate forest. *J. Geophys. Res.: Biogeosciences* 125 (12), <http://dx.doi.org/10.1029/2020JG005892>.
- Zarakas, C.M., Kennedy, D., Dagon, K., Lawrence, D.M., Liu, A., Bonan, G., Koven, C., Lombardozzi, D., Swann, A.L.S., 2024. Land processes can substantially impact the mean climate state. *Geophys. Res. Lett.* 51 (21), <http://dx.doi.org/10.1029/2024GL108372>.
- Zhang, B., Hautier, Y., Tan, X., You, C., Cadotte, M.W., Chu, C., Jiang, L., Sui, X., Ren, T., Han, X., Chen, S., 2020. Species responses to changing precipitation depend on trait plasticity rather than trait means and intraspecific variation. *Funct. Ecol.* 34 (12), 2622–2633. <http://dx.doi.org/10.1111/1365-2435.13675>.
- Zhang, K., Kimball, J.S., Running, S.W., 2016. A review of remote sensing based actual evapotranspiration estimation. *Wiley Interdiscip. Rev.: Water* 3 (6), 834–853. <http://dx.doi.org/10.1002/wat2.1168>.
- Zhou, S., Zhang, Y., Park Williams, A., Gentine, P., 2019. Projected increases in intensity, frequency, and terrestrial carbon costs of compound drought and aridity events. *Sci. Adv.* 5 (1), eaau5740. <http://dx.doi.org/10.1126/sciadv.aau5740>.
- Zhu, L., Bloomfield, K.J., Hocart, C.H., Egerton, J.J., O'Sullivan, O.S., Penillard, A., Weerasinghe, L.K., Atkin, O.K., 2018. Plasticity of photosynthetic heat tolerance in plants adapted to thermally contrasting biomes. *Plant, Cell & Environ.* 41 (6), 1251–1262. <http://dx.doi.org/10.1111/pce.13133>.